

A RECTANGULAR BILLIARD WITH MOVING SLITS

JING ZHOU

ABSTRACT. We describe an exponential Fermi accelerator in a two-dimensional billiard with a moving slit. We have found a mechanism of trapping regions which provides the exponential acceleration for almost all initial conditions with sufficiently high initial energy. Under an additional hyperbolicity assumption, we estimate the waiting time after which most high-energy orbits start to gain energy exponentially fast.

1. INTRODUCTION

In an attempt to explain the existence of high energy particles in cosmic rays, Fermi [8] in 1949 proposed a model in which charged particles undergo repeated reflections in moving magnetic fields. Later in 1961 Ulam [26] proposed that a similar mechanism should appear in finite degree of freedom systems. He described a toy model where a particle bounces elastically between two walls, one fixed and the other moving periodically. Ulam [26] performed numerical experiments on a piecewise linear model and conjectured that there exist escaping orbits whose energy tend to infinity with time. Since then extensive efforts have been made by both mathematicians and physicists to locate escaping orbits in various settings (see [18, 6, 10] for surveys on this subject).

Notably the KAM theory has eliminated the possibility of such escaping orbits in one-dimensional Fermi-Ulam model for sufficiently smooth wall motions [16] [23] [24], as the prevalence of invariant curves forces all orbits to be bounded. However, unbounded solution can still be obtained in nonsmooth case. For example, Zharnitsky [27] has found a type of unbounded orbits in the Ulam's piecewise linear case, which

Date: July 30, 2019.

The author thanks Vered Rom-Kedar for posing this problem and for many useful discussions on this subject. The author is also much obliged to Dmitry Dolgopyat for enlightening comments and advice. The research was partially supported by NSF grant DMS 1665046 and by BSF grant 2016105. Part of this work was done at Weizmann Institute, where the hospitality and excellent working conditions are gratefully acknowledged.

grows linearly with time. In a one-dimensional Fermi-Ulam model with one discontinuity, De Simoi and Dolgopyat [3] has showed that there exists a parameter that completely shapes the large energy behavior of the system: in the hyperbolic regime the escaping set has zero measure but full Hausdorff dimension while in some elliptic cases the escaping orbits have infinite measure. There are many interesting question pertaining to Fermi-Ulam model with non-periodic wall motion. We refer the reader to [28, 15] for the results in quasi-periodic case. One and a half degree of freedom models where the motion between collision is not free but is subjected to a potential are discussed, for example in [22, 20, 21, 5, 2, 1].

Two-dimensional moving billiard models are natural generalization of the one-dimensional Fermi acceleration model and can often provide chaotic orbits even in the smooth case. For example, unbounded orbits were found in billiard models with the smoothly breathing boundary [13, 14, 17]. In a Lorentz gas model [19], the average velocity of particles grows linearly in time for stochastic perturbation of scatterer boundaries and quadratically for periodic perturbation. Exponential growing orbits for non-autonomous billiards were constructed in [12] but in general it remains challenging to detect a positive measure set of exponentially growing orbits. Exponential acceleration is also conjectured to be generic for oscillating mushrooms [11]. The models which are closest to our setting are the following. Shah, Turaev and Rom-Kedar [25] investigated a rectangular billiard model with a moving slit. They proposed a random process approximation for the particle energy from which the calculated exponential growth rate agrees well with the numerical results for typical trajectories in the non-resonant case. They also observed numerically in [25] that the growth rate in the resonant case is significantly higher than that in the non-resonant case. Later they generalized the idea to higher-dimensional time-dependent billiards and obtained a new class of numerically robust exponential accelerators [9]. The model presented in this paper was inspired by their work.

We study a rectangular billiard with two moving slits. In our model, the billiard table is a unit square. Two slits are moving vertically in the table with the length of left slit λ and the length of the right slit $1 - \lambda$, where $\lambda \in (0, 1)$ is a constant. The motion of the two slits are described by two C^2 2-periodic functions $f_L(t)$ and $f_R(t)$ respectively. A massless ball bounces elastically against the moving slits as well as

the boundary of the rectangular table.

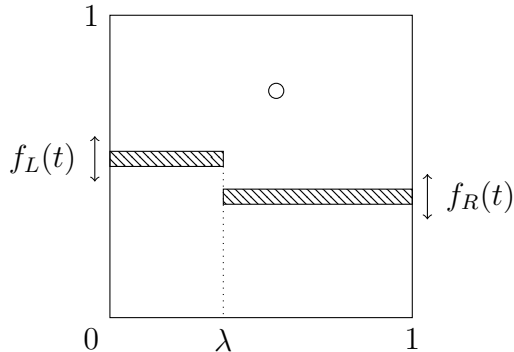


FIGURE 1. Rectangular Billiard with Moving Slits

In this paper we study the simplest resonant case. Namely, we assume that the horizontal speed the ball is 1, so the horizontal coordinate of the ball is periodic with period 2. Hence we have 1:1 resonance between the period of moving slits and the period the horizontal motion of the ball. The ball experiences two jumps between the left and the right parts of the table during each period. We denote by x_0 the starting horizontal position of the ball. We assume without loss of generality that the ball starts from the left part, i.e. $0 \leq x_0 < \lambda$. The ball jumps from the left slit to right one at time $t_1^* = \lambda - x_0$ and then from right to the left at time $t_2^* = 2 - \lambda - x_0$.

We record the time and the vertical velocity of the ball immediately after each collision with the slits. We exclude from our discussion the trajectories having a collision at $x = \lambda$. The excluded orbits constitute a measure zero set among all the initial conditions.

We describe in this paper a new exponential accelerator. We show that almost all initial conditions with sufficiently high initial velocity produce exponential energy growth in the future, provided that the relative positions of the two slits change at the time of the two jumps between left and right parts of the table. Moreover, under an additional hyperbolicity assumption we estimate the waiting time after which most high-energy orbits start to accelerate exponentially.

2. MAIN RESULTS

In this section we describe the exponential accelerator we have found. For a wide range of choices in λ and x_0 , the relative positions of the left

and right slits change when the ball jumps from one slit to the other at time t_1^* and t_2^* (c.f. Figure 2). A trapping region is created in this case and the ball starts to gain energy exponentially fast once it gets trapped.

Theorem 1. *Assume that $f_L(t_1^*) < f_R(t_1^*)$ and $f_L(t_2^*) > f_R(t_2^*)$ or $f_L(t_1^*) > f_R(t_1^*)$ and $f_L(t_2^*) < f_R(t_2^*)$. Then there exists $V_* \gg 1$, which depends only on f_L and f_R , such that almost every orbit whose initial speed is greater than V_* eventually gains energy exponentially in time. In particular, the set of initial conditions (t_0, v_0) which do not enjoy exponential energy growth has finite measure.*

In the presence of a trapping region, with additional hyperbolicity assumptions we estimate the waiting time after which most high-energy orbits start to accelerate exponentially.

We define a new function f as follows

$$f(t) = \begin{cases} f_L(t) & 0 < t < t_1^* \text{ or } t_2^* < t < 2 \\ f_R(t) & t_1^* < t < t_2^*. \end{cases}$$

We introduce a new quantity Tr . If the lower chamber is trapping, then we define in the upper chamber

$$Tr^U = \left(\frac{1 - f_1^-}{1 - f_1^+} - a_1 \beta \right) \left(\frac{1 - f_2^-}{1 - f_2^+} - a_2 \alpha \right) + \left(\frac{1 - f_1^+}{1 - f_1^-} - a_1 \alpha \right) \left(\frac{1 - f_2^+}{1 - f_2^-} - a_2 \beta \right) - a_1 a_2 \alpha \beta$$

where $f_i^\pm = f(t_i^* \pm)$, $a_i = \dot{f}_i^-(1 - f_i^+) - \dot{f}_i^+(1 - f_i^-)$,

$$\alpha = \left(\int_0^{t_1^*} + \int_{t_2^*}^2 \right) \frac{ds}{(1 - f(s))^2} \quad \text{and} \quad \beta = \int_{t_1^*}^{t_2^*} \frac{ds}{(1 - f(s))^2}.$$

If the upper chamber is trapping, then we define in the lower chamber

$$Tr^L = \left(\frac{f_1^-}{f_1^+} - a'_1 \beta' \right) \left(\frac{f_2^-}{f_2^+} - a'_2 \alpha' \right) + \left(\frac{f_1^+}{f_1^-} - a'_1 \alpha' \right) \left(\frac{f_2^+}{f_2^-} - a'_2 \beta' \right) - a'_1 a'_2 \alpha' \beta'$$

where $a'_i = \dot{f}_i^+ f_i^- - \dot{f}_i^- f_i^+$, $\alpha' = \left(\int_0^{t_1^*} + \int_{t_2^*}^2 \right) \frac{ds}{f(s)^2}$ and $\beta' = \int_{t_1^*}^{t_2^*} \frac{ds}{f(s)^2}$.

Theorem 2. *Assume λ and x_0 are such that the relative positions of two slits change at two critical jumps and that $|Tr| > 2$. Then there is $K, \zeta > 0$ such that for any $\epsilon > 0$, there exists $V_0 = V_0(\epsilon)$ and $T = T(\epsilon)$ such that for each $V \geq V_0$ the complement of set*

$$\left\{ (t_0, v_0) : |v_0| \in [V, V + 1] : \forall t \geq T \quad |v(t)| \geq \frac{|v(T)|}{K} e^{\zeta t} \right\}$$

has measure less than ϵ , i.e. most orbits with initial energy $|v_0| > V_0$ start to accelerate exponentially after time T .

The proof of this result is constructive. In particular, T depends logarithmically on ϵ (see equations (12) and (13)).

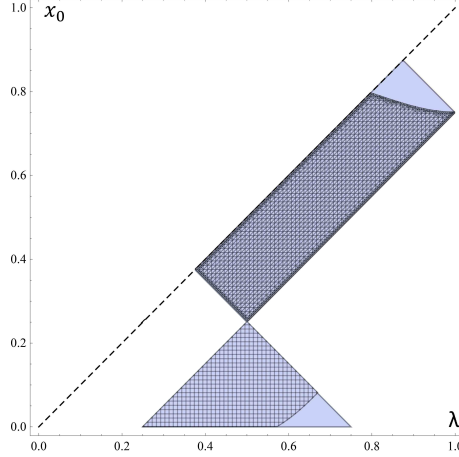


FIGURE 2. Trapping Regions

The plot of trapping regions for $f_L(t) = 0.3 \cos(\pi t) + 0.5$, $f_R(t) = 0.3 \sin(\pi t) + 0.5$. The blue part indicates the values of λ, x_0 for which a trapping region exists: the upper rectangle is where the upper chamber is trapping and the lower triangle is where the lower chamber is trapping. The shaded part displays where the hyperbolicity assumption $|Tr| > 2$ holds.

Example 2.1. To illustrate our results, we consider the case where

$$(1) \quad f_L(t) = 0.3 \cos(\pi t) + 0.5, \quad f_R(t) = 0.3 \sin(\pi t) + 0.5.$$

Then

$$\Delta(t) := f_L(t) - f_R(t) = 0.3\sqrt{2} \cos\left(\pi t + \frac{\pi}{4}\right).$$

A trapping region exists for λ, x_0 such that either

$$\Delta(\lambda - x_0) > 0, \quad \Delta(2 - \lambda - x_0) < 0 \quad \text{or} \quad \Delta(\lambda - x_0) < 0, \quad \Delta(2 - \lambda - x_0) > 0.$$

The former case is equivalent to $\lambda - x_0 < 0.25$, $0.75 < \lambda + x_0 < 1.75$; the upper chamber is trapping and the hyperbolicity assumption holds if $|Tr^L| > 2$.

The latter case is equivalent to $\lambda - x_0 > 0.25$, $\lambda + x_0 < 0.75$; the lower chamber is trapping and the hyperbolicity assumption holds if $|Tr^U| > 2$.

Figure 2 demonstrates that for f_L, f_R defined above by (1) the assumptions of Theorems 1 and 2 hold for a sizable set of parameters.

The structure of the rest of the paper is the following. In Section 3 we describe the collision map. In Section 4 we derive the normal form for the map obtained by considering the next collision with the moving wall after the ball switches from left to right chamber or *vice versa*. The proof of Theorem 1 is given in Section 5 and the proof of Theorem 2 is given in Section 6. In Section 7 we summarize the tools developed in the present paper and discuss open problems.

3. PRELIMINARIES

Since the horizontal speed of the ball stays constant, only the vertical speed contributes to the energy change of the ball. This is why we only need to record the time t and the vertical velocity v immediately after each collision. Let us denote by F the collision map.

For $i = 1, 2$, we denote as R_i the strip in the (t, v) -plane bounded by the singularity line $\mathcal{S}_i = \{t = t_i^*\}$ and its image $F\mathcal{S}_i$. Also let $\tilde{R}_i = F^{-1}R_i$. We subdivide the singular strips R into upper and lower chamber parts R^+ and R^- .

There are four possible scenarios when the ball makes a jump: the ball always hits the slits from above or below, the ball first hits from above then from below and vice versa.

We start with the easiest case when the ball always stays in the same chamber. Then the system is effectively equivalent to a Fermi-Ulam model with the motion (height) of the wall being the piecewise smooth 2-periodic function $f(t)$ with two jump discontinuities at t_1^* and t_2^* .

Suppose that the ball is initially in the upper chamber. We omit the subscript i as the formulas for passing through the two singularities are the same. If for $(t, v) \in \tilde{R}$ we have $f(t^*+) - f(t) < v(t^* - t) < 2 - f(t) - f(t^*)$, then the ball ends in the upper chamber after jumping and the model is equivalent to the one with a fixed ceiling and a moving floor (c.f. Figure 3 on the left).

Two consecutive collisions (t_n, v_n) and $(t_{n+1}, v_{n+1}) = F(t_n, v_n)$ satisfy

$$(2) \quad \begin{cases} v_{n+1} = v_n + 2\dot{f}(t_{n+1}) \\ 2 - f(t_n) - f(t_{n+1}) = v_n(t_{n+1} - t_n). \end{cases}$$

Similarly, suppose that the ball is initially in the lower chamber. If for $(t, v) \in \tilde{R}$ we have $f(t) - f(t^*+) < -v(t^* - t) < f(t) + f(t^*)$, then the ball ends in the lower chamber after jumping and the model is equivalent to the one with a moving ceiling and a fixed floor (c.f.

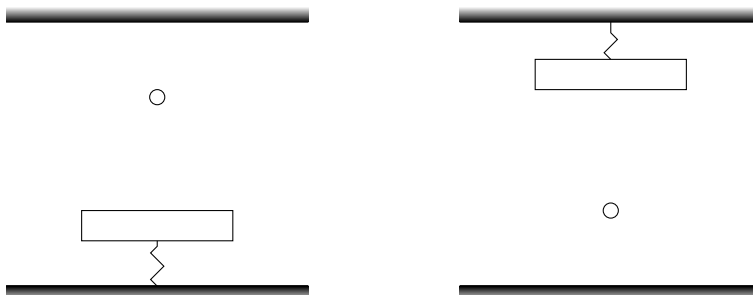


FIGURE 3. Equivalent Fermi-Ulam Models for the Upper/Lower Chambers

Figure 3 on the right). Two consecutive collisions satisfy

$$(3) \quad \begin{cases} v_{n+1} = v_n + 2\dot{f}(t_{n+1}) \\ f(t_n) + f(t_{n+1}) = -v_n(t_{n+1} - t_n). \end{cases}$$

Now let us examine the switching cases.

Suppose that the ball is initially in the upper chamber and two consecutive collisions still follow Equation (2) before the ball jumps from one slit to the other. However, when the ball jumps, if the next chamber is above the previous one when the ball passes through the singularities, then there is a possibility that the ball enters the lower chamber. More precisely, for $(t, v) \in \tilde{R}$, if $v(t_* - t) > 2 - f(t) - f(t_*+)$, then the ball collides with the ceiling and then enters the lower chamber (c.f. Figure 4 on the left); while if $v(t_* - t) < f(t_*+) - f(t)$, then the ball enters the lower chamber immediately after it leaves the previous slit (c.f. Figure 4 on the right).

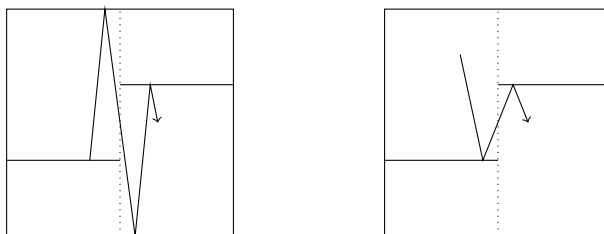


FIGURE 4. From Upper to Lower Cases

Two consecutive collisions satisfy the following Equation (4) in the first case

$$(4) \quad \begin{cases} v_n(t_{n+1} - t_n) = f(t_{n+1}) - f(t_n) + 2 \\ v_{n+1} = -v_n + 2\dot{f}(t_{n+1}) \end{cases}$$

and the following Equation (5) in the second case

$$(5) \quad \begin{cases} v_n(t_{n+1} - t) = f(t_{n+1}) - f(t_n) \\ v_{n+1} = -v_n + 2\dot{f}(t_{n+1}). \end{cases}$$

On the other hand, suppose the ball is initially in the lower chamber and two consecutive collisions still follow Equation (3) before the ball jumps from one slit to the other. When the ball jumps, if the next chamber is below the previous one when the ball passes through the singularities, then there is a possibility that the ball enters the upper chamber. More precisely, for $(t, v) \in \tilde{R}$, if $-v(t_* - t) > f(t) + f(t_* -)$, then the ball collides with the floor and enters the upper chamber (c.f. Figure 5 on the left); while if $-v(t_* - t) < f(t) - f(t_* -)$, then the ball enters the lower chamber immediately after it leaves the previous slit (c.f. Figure 5 on the right).

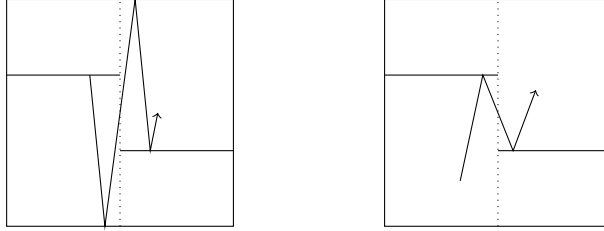


FIGURE 5. From Lower to Upper Cases

Two consecutive collisions satisfy the following Equation (6) in the first case

$$(6) \quad \begin{cases} v_n(t_{n+1} - t_n) = f(t_{n+1}) - f(t_n) - 2 \\ v_{n+1} = -v_n + 2\dot{f}(t_{n+1}) \end{cases}$$

and the following Equation (7) in the second case

$$(7) \quad \begin{cases} v_n(t_{n+1} - t) = f(t_{n+1}) - f(t_n) \\ v_{n+1} = -v_n + 2\dot{f}(t_{n+1}). \end{cases}$$

4. THE NORMAL FORM

In this section we study how the (vertical) velocity of the ball changes after one period $\Delta t = 2$ given sufficiently large initial energy. We will first approximate the collision map F with an action-angle coordinate away from singularities. Then we examine the collision dynamics when the ball passes through singularities.

4.1. The Action-Angle Coordinate. First we suppose that the ball collides with the slit from above and it does not make a jump at nearby collisions.

Let us denote $l(t) = 1 - f(t)$ and $\mathcal{L}_* = \int_0^2 l^{-2}(s) ds$.

Lemma 4.1. *For $(t, v) \notin R_i \cup \tilde{R}_i$ ($i = 1, 2$) and $v \gg 1$, there exists an action-angle coordinate $(\theta, I) = \Psi_U(t, v) \in \mathbb{R}/2\mathbb{Z} \times \mathbb{R}_+$ such that*

$$\theta_{n+1} = \theta_n + \frac{2}{I_n} + \mathcal{O}\left(\frac{1}{I_n^4}\right), \quad I_{n+1} = I_n + \mathcal{O}\left(\frac{1}{I_n^3}\right).$$

In fact, $\theta = \theta(t) = \frac{2}{\mathcal{L}_*} \int_0^t \frac{ds}{l(s)^2} \pmod{2}$, $I = I(t, v) = \frac{\mathcal{L}_*}{2} \left(lv + l\dot{l} + \frac{l^2\ddot{l}}{3v} \right)$.

Proof. We can check the formula by a direct computation (c.f. Lemma 2.2 in [3]), or we can derive it in an inductive way (c.f. Section 2.2 in [4]). The basic idea is to find higher-order adiabatic invariants. For example, observe that

$$v_{n+1} - v_n \approx -2\dot{l}(t_n), \quad t_{n+1} - t_n \approx \frac{2l(t_n)}{v_n}.$$

This leads to the Euler scheme of the following ODE

$$\frac{dv}{dt} = \frac{-v\dot{l}}{l}$$

which in turn gives us the zeroth order adiabatic invariant $I = lv$. Then we update the scheme by replacing v with I and look for the first order adiabatic invariant, etc. This scheme terminates at the second order adiabatic invariant $I = lv + l\dot{l} + \frac{l^2\ddot{l}}{3v}$.

Next, the formula for θ can be obtained reversely by solving the ODE

$$\theta' \frac{2l}{v} = \frac{2}{lv}$$

which leads to $\theta(t) = \int_0^t l^{-2}(s) ds$.

We observe that only the order v term in I is used to derive the formula

for θ and it seems to produce an estimate only up to first order

$$\theta_{n+1} - \theta_n = 2/I_n + \mathcal{O}(I_n^{-2}).$$

But in fact by noting the Taylor expansion of l^{-2} and that

$$t_{n+1} - t_n = \frac{2l(t_n)}{v_n} + \frac{2l(t_n)\dot{l}(t_n)}{v_n^2} + \frac{2l(t_n)\dot{l}(t_n)^2 + 2l(t_n)^2\ddot{l}(t_n)}{v_n^3} + \mathcal{O}(v_n^{-4})$$

we obtain that

$$\begin{aligned} \int_{t_n}^{t_{n+1}} l^{-2}(s) ds &= \frac{t_{n+1} - t_n}{l_n^2} - \frac{\dot{l}_n}{l_n^3} (t_{n+1} - t_n)^2 + \left(\frac{\dot{l}_n^2}{l_n^4} - \frac{\ddot{l}_n}{3l_n^3} \right) (t_{n+1} - t_n)^3 + \mathcal{O}(v_n^{-4}) \\ &= \frac{2}{l_n v_n} - \frac{2\dot{l}_n}{t_n v_n^2} + \frac{2\dot{l}_n^2 - \frac{2}{3}l_n \ddot{l}_n}{l_n v_n^3} + \mathcal{O}(v_n^{-4}) \\ &= \frac{2}{I_n} + \frac{2\dot{l}_n}{v_n I_n} + \frac{2l_n \ddot{l}_n}{3v_n^2 I_n} - \frac{2\dot{l}_n}{l_n v_n^2} + \frac{2\dot{l}_n^2 - \frac{2}{3}l_n \ddot{l}_n}{l_n v_n^3} + \mathcal{O}(v_n^{-4}) \\ &= \frac{2}{I_n} + \frac{2\dot{l}_n^2}{v_n^2 I_n} + \frac{2l_n \ddot{l}_n}{3v_n^2 I_n} + \frac{2\dot{l}_n^2 - \frac{2}{3}l_n \ddot{l}_n}{l_n v_n^3} + \mathcal{O}(v_n^{-4}) \\ &= \frac{2}{I_n} + \mathcal{O}(v_n^{-4}) \end{aligned}$$

where $l_n = l(t_n)$ and $\dot{l}_n = \dot{l}(t_n)$, which produces the desired third order estimate.

Finally, we need to rescale θ (and hence I) to make θ 2 periodic. \square

Next we assume that the ball collides at the slits from below and it does not make a jump at nearby collisions.

We introduce a new function $g(t) = f(t) + 1$. Then Equation (3) becomes the same as Equation (2) with g in place of f

$$(8) \quad \begin{cases} v_{n+1} = v_n + 2\dot{g}(t_{n+1}) \\ 2 - g(t_n) - g(t_{n+1}) = v_n(t_{n+1} - t_n) \end{cases}$$

Therefore all the computation above in Lemma 4.1 applies with g in the place of f .

We define $m(t) = 1 - g(t) = -f(t)$ and $\mathcal{M}_* = \int_0^2 m(s)^{-2} ds$. We have an action-angle coordinate if the collision occurs in the lower chamber away from singularities

Lemma 4.2. *For $(t, v) \notin R_i \cup \tilde{R}_i$ ($i = 1, 2$) and $v \ll -1$, there exists an action-angle coordinate $(\zeta, J) = \Psi_L(t, v) \in \mathbb{R}/2\mathbb{Z} \times \mathbb{R}_+$ such that*

$$\zeta_{n+1} = \zeta_n + \frac{2}{J_n} + \mathcal{O}\left(\frac{1}{J_n^4}\right), \quad J_{n+1} = J_n + \mathcal{O}\left(\frac{1}{J_n^3}\right).$$

In fact, $\zeta = \zeta(t) = \frac{2}{\mathcal{M}_*} \int_0^t \frac{ds}{m(s)^2} \pmod{2}$, $J = J(t, v) = \frac{\mathcal{M}_*}{2} \left(mv + m\dot{m} + \frac{m^2\ddot{m}}{3v} \right)$.

4.2. The Normal Forms. In this section we present the Poincaré map P from one singular strip to the other in four possible scenarios. We assume the initial energy of the ball is sufficiently large $|v_0| > V_*$ for some large V_* in all the cases.

4.2.1. The Upper-Upper Chamber Case. We begin with the upper-upper chamber case, i.e. the ball stays in the upper chamber both before and after it makes a jump. Lemma 4.1 already depicts the dynamics away from singularities. Now let us scrutinize what occurs near the singularities t_i^* ($i = 1, 2$) when the ball makes a jump.

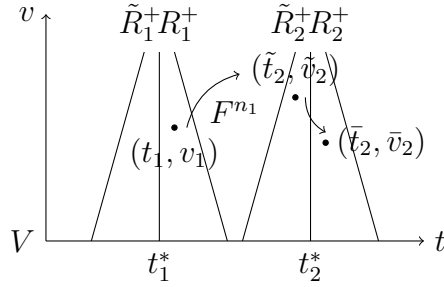


FIGURE 6. The Poincaré Map P_{UU}^{12} on the Singular Strips

For $(t_1, v_1) \in R_1^+$ with $v_1 > V_*$, we denote $(\tilde{t}_2, \tilde{v}_2) = F^{n_1}(t_1, v_1) \in \tilde{R}_2^+$, where $n_1 = [\frac{I_1}{2}(\theta_2^* - \theta_1)]$ and $\theta_2^* = \frac{2}{\mathcal{L}_*} \int_0^{t_2^*} \frac{ds}{l(s)^2}$, and $(\bar{t}_2, \bar{v}_2) = F(\tilde{t}_2, \tilde{v}_2) \in R_2^+$. Similarly, for $(t_2, v_2) \in R_2^+$ with $v_2 \gg 1$, we denote $(\tilde{t}_1, \tilde{v}_1) = F^{n_2}(t_2, v_2) \in \tilde{R}_1^+$, where $n_2 = [\frac{I_2}{2}(2 + \theta_1^* - \theta_2)]$ and $\theta_1^* = \frac{2}{\mathcal{L}_*} \int_0^{t_1^*} \frac{ds}{l(s)^2}$, and $(\bar{t}_1, \bar{v}_1) = F(\tilde{t}_1, \tilde{v}_1) \in R_1^+$.

We introduce a new pair of variables (τ, \mathcal{I}) defined on the upper singular strips

$$\tau = \begin{cases} I(\theta - \theta_1^*) & \text{on } R_1^+ \\ I(\theta - \theta_2^*) & \text{on } R_2^+ \end{cases}, \quad \mathcal{I} = \frac{I}{\mathcal{L}_*} \text{ on } R_1^+, R_2^+$$

Now we present the Poincaré maps $P_{UU}^{12} : R_1^+ \rightarrow R_2^+$ and $P_{UU}^{21} : R_2^+ \rightarrow R_1^+$ which captures the collision dynamics when the ball travels from one singular strips to the other. We need the following constants ($i =$

1, 2):

$$\begin{aligned}\Delta_i &= \frac{1}{2} \frac{l(t_i^*+)}{l(t_i^*-)} \left(l(t_i^*-)\dot{l}(t_i^*+) - l(t_i^*+)\dot{l}(t_i^*-) \right), \\ \Delta'_i &= \frac{1}{8} l(t_i^*+)^2 \left(l(t_i^*-)\ddot{l}(t_i^*+) - l(t_i^*+)\ddot{l}(t_i^*-) \right), \\ \Delta''_i &= \frac{1}{24} l(t_i^*-)l(t_i^*+) \left(l(t_i^*-)\dddot{l}(t_i^*+) - l(t_i^*+)\dddot{l}(t_i^*-) \right).\end{aligned}$$

Proposition 4.3 (Upper-Upper). *Suppose that $(\tau_1, \mathcal{I}_1) \in R_1^+$ and $\mathcal{I}_1 > V_*$, and that*

$$f(t_2^*+) - f(t_2^*-) \lesssim l_2^- \{ \mathcal{L}_* \mathcal{I}_1 (\theta_2^* - \theta_1^*) - \tau_1 \}_2 \lesssim 2 - f(t_2^*+) - f(t_2^*-),$$

where \lesssim means the inequality holds up to an error of order $\mathcal{O}(\frac{1}{\mathcal{I}_1})$, and $\{\bullet\}_2 = \bullet \pmod{2}$. Then the Poincaré map $P_{UU}^{12} : R_1^+ \rightarrow R_2^+$ is given by $(\bar{\tau}_2, \bar{\mathcal{I}}_2) = G_{UU}^{12}(\tau_1, \mathcal{I}_1) + H_{UU}^{12}(\tau_1, \mathcal{I}_1) + \mathcal{O}(\mathcal{I}_1^{-2})$ where

$$G_{UU}^{12}(\tau_1, \mathcal{I}_1) = \left(-\frac{l_2^-}{l_2^+} \{ \mathcal{L}_* \mathcal{I}_1 (\theta_2^* - \theta_1^*) - \tau_1 \}_2 + 1 + \frac{l_2^-}{l_2^+}, \frac{l_2^-}{l_2^+} \mathcal{I}_1 + \Delta_2(\bar{\tau}_2 - 1) \right)$$

and

$$H_{UU}^{12}(\tau_1, \mathcal{I}_1) = (0, \Delta'_2(\bar{\tau}_2 - 1)^2/\mathcal{I}_1 + \Delta''_2/\mathcal{I}_1)$$

Similarly, suppose that $(\tau_2, \mathcal{I}_2) \in R_2^+$, $\mathcal{I}_2 > V_*$, and that

$$f(t_1^*+) - f(t_1^*-) \lesssim l_1^- \{ \mathcal{L}_* \mathcal{I}_2 (2 + \theta_1^* - \theta_2^*) - \tau_2 \}_2 \lesssim 2 - f(t_1^*+) - f(t_1^*-).$$

Then the Poincaré map $P_{UU}^{21} : R_2^+ \rightarrow R_1^+$ is given by

$$(\bar{\tau}_1, \bar{\mathcal{I}}_1) = G_{UU}^{21}(\tau_2, \mathcal{I}_2) + H_{UU}^{21}(\tau_2, \mathcal{I}_2) + \mathcal{O}(\mathcal{I}_2^{-2})$$

where

$$G_{UU}^{21}(\tau_2, \mathcal{I}_2) = \left(-\frac{l_1^-}{l_1^+} \{ \mathcal{L}_* \mathcal{I}_2 (2 + \theta_1^* - \theta_2^*) - \tau_2 \}_2 + 1 + \frac{l_1^-}{l_1^+}, \frac{l_1^-}{l_1^+} \mathcal{I}_2 + \Delta_1(\bar{\tau}_1 - 1) \right),$$

$$H_{UU}^{21}(\tau_2, \mathcal{I}_2) = (0, \Delta'_1(\bar{\tau}_1 - 1)^2/\mathcal{I}_2 + \Delta''_1/\mathcal{I}_2)$$

and $l_i^\pm = l(t_i^*\pm)$.

Proof. We only derive the formula for P_{UU}^{12} . The formula for P_{UU}^{21} can be obtained in a similar fashion.

For the ease of notation we drop the sub/superscripts whenever they are clear from the context. Note that near the jump discontinuity at

t^*

$$\begin{aligned}
l(\tilde{t}^*) &= l_-(t^*) + \dot{l}_-(\tilde{t} - t^*) + \frac{1}{2}\ddot{l}_-(t^*)(\tilde{t} - t^*)^2 + \mathcal{O}(\tilde{v}^{-3}), \\
l(\bar{t}^*) &= l_+(t^*) + \dot{l}_+(\bar{t} - t^*) + \frac{1}{2}\ddot{l}_+(t^*)(\bar{t} - t^*)^2 + \mathcal{O}(\tilde{v}^{-3}), \\
\dot{l}(\tilde{t}^*) &= \dot{l}_-(t^*) + \ddot{l}_-(\tilde{t} - t^*) + \mathcal{O}(\tilde{v}^{-2}), \\
\dot{l}(\bar{t}^*) &= \dot{l}_+(t^*) + \ddot{l}_+(\bar{t} - t^*) + \mathcal{O}(\tilde{v}^{-2}), \\
\ddot{l}(\tilde{t}^*) &= \ddot{l}_-(t^*) + \mathcal{O}(\tilde{v}^{-1}), \\
\ddot{l}(\bar{t}^*) &= \ddot{l}_+(t^*) + \mathcal{O}(\tilde{v}^{-1}),
\end{aligned}$$

and that

$$\bar{v} = \tilde{v} - 2\dot{l}(\bar{t}), \quad \bar{t} - \tilde{t} = \frac{l(\bar{t}) + l(\tilde{t})}{\bar{v}}.$$

Hence by solving iteratively the implicit equation we attain

$$\bar{t} - \tilde{t} = \frac{l_+ + l_-}{\tilde{v}} + (\dot{l}_+ + \dot{l}_-)\frac{\bar{t} - t^*}{\tilde{v}} - \frac{\dot{l}_-(l_+ + l_-)}{\tilde{v}^2} + \mathcal{O}(\tilde{v}^{-3}).$$

By a straightforward but tedious computation we arrive at

$$\begin{aligned}
2\mathcal{L}_*^{-1} \left(\frac{l_-}{l_+} \bar{I} - \tilde{I} \right) &= (l_+ \dot{l}_- - l_- \dot{l}_+) - \frac{l_+ \dot{l}_- - l_- \dot{l}_+}{l_+} (\bar{t} - t^*) \bar{v} \\
&\quad + (l_+ \ddot{l}_- - l_- \ddot{l}_+ + \frac{l_-}{l_+} \dot{l}_+^2 - \dot{l}_- \dot{l}_+) (\bar{t} - t^*) \\
&\quad + \left(\frac{l_-}{3} (l_+ \ddot{l}_+ - l_- \ddot{l}_-) + \frac{\dot{l}_-}{2} (l_-^2 - l_+^2) \right) \frac{1}{\bar{v}} \\
&\quad - \frac{l_+ \ddot{l}_- - l_- \ddot{l}_+}{2l_+} (\bar{t} - t^*)^2 \bar{v} + \mathcal{O}(\tilde{v}^{-2}) \\
&= \frac{l_- \dot{l}_+ - l_+ \dot{l}_-}{l_+} \left((\bar{t} - t^*) \bar{v} \left(1 + \frac{\dot{l}_+}{\bar{v}} \right) - l_+ \right) \\
&\quad + \frac{l_- \ddot{l}_+ - l_+ \ddot{l}_-}{2l_+ \bar{v}} \left(((\bar{t} - t^*) \bar{v} - l_+)^2 + \frac{l_- l_+ (l_- \ddot{l}_- - l_+ \ddot{l}_+)}{3(l_- \ddot{l}_+ - l_+ \ddot{l}_-)} \right) + \mathcal{O}(\tilde{v}^{-2}).
\end{aligned}$$

It can be checked directly by Taylor expanding \bar{I} and $\bar{\theta}$ that

$$\bar{\tau} = \bar{I}(\bar{\theta} - \theta_2^*) = \frac{1}{l_+} \left((\bar{t} - t^*) \bar{v} + \dot{l}_+(\bar{t} - t^*) \right) + \mathcal{O}(\tilde{v}^{-2}).$$

Thus eventually we have

$$\bar{\mathcal{I}} = (l_+/l_-)\tilde{\mathcal{I}} + \Delta(\bar{\tau} - 1) + \Delta'(\bar{\tau} - 1)^2/\tilde{\mathcal{I}} + \Delta''/\tilde{\mathcal{I}} + \mathcal{O}(\tilde{\mathcal{I}}^{-2}).$$

Now we compute $\bar{\tau}$. Observe that

$$\bar{\tau} = \frac{\bar{v} + \dot{l}_+}{l_+}(\bar{t} - t^*) + \mathcal{O}(\bar{v}^{-2}), \quad \tilde{I}(\tilde{\theta} - \tilde{\theta}_2^*) = \frac{\tilde{v} + \dot{l}_-}{l_-}(\tilde{t} - t^*) + \mathcal{O}(\bar{v}^{-2}).$$

Therefore

$$\begin{aligned} l_+ \bar{\tau} &= ((\bar{t} - \tilde{t}) + (\tilde{t} - t^*))(\tilde{v} + \dot{l}_- - (\dot{l}_- + \dot{l}_+)) + \mathcal{O}(\tilde{v}^{-2}) \\ &= (\tilde{t} - t^*)(\tilde{v} + \dot{l}_-) + (\bar{t} - \tilde{t})(\tilde{v} + \dot{l}_-) - (\bar{t} - t^*)(\dot{l}_- + \dot{l}_+) + \mathcal{O}(\tilde{v}^{-2}) \\ &= l_- \tilde{I}(\tilde{\theta} - \tilde{\theta}_2^*) + \frac{l_- + l_+}{\tilde{v}}(\tilde{v} + \dot{l}_-) + (\dot{l}_- + \dot{l}_+)(\bar{t} - t^*) \\ &\quad - \frac{\dot{l}_-(l_- + l_+)}{\tilde{v}} - (\bar{t} - t^*)(\dot{l}_- + \dot{l}_+) + \mathcal{O}(\tilde{v}^{-2}) \\ &= l_- \tilde{I}(\tilde{\theta} - \tilde{\theta}_2^*) + l_- + l_+ + \mathcal{O}(\tilde{v}^{-2}), \end{aligned}$$

which gives

$$\bar{\tau} = (l_-/l_+) \tilde{I}(\tilde{\theta} - \tilde{\theta}_2^*) + 1 + l_-/l_+ + \mathcal{O}(\tilde{I}^{-2}).$$

But Lemma 4.1 implies that

$$\tilde{I} = I + \mathcal{O}(I^{-2}), \quad \tilde{\theta} = \theta + \frac{2n_1}{I} + \mathcal{O}(I^{-3})$$

hence we have

$$\tilde{I}(\tilde{\theta} - \tilde{\theta}_2^*) = \tau + 2n_1 + I(\theta_1^* - \theta_2^*) + \mathcal{O}(I^{-2})$$

where $n_1 = [\frac{I_1}{2}(\theta_2^* - \theta_1)]$.

We hitherto complete the proof of the formula for P_{UV}^{12} . \square

4.2.2. The Lower-Lower Chamber Case. We present here the mirror case to Section 4.2.1, i.e. when the ball stays in the lower chamber both before and after it makes a jump.

We need the following constants ($i = 1, 2$)

$$\begin{aligned} \zeta_i^* &= \frac{2}{M_*} \int_0^{t_i^*} m(s)^{-2} ds \\ \Upsilon_i &= \frac{1}{2} \frac{m_i^+}{m_i^-} (m_i^- \dot{m}_i^+ - m_i^+ \dot{m}_i^-) \\ \Upsilon_i' &= \frac{1}{8} m_i^{+2} (m_i^- \ddot{m}_i^+ - m_i^+ \ddot{m}_i^-) \\ \Upsilon_i'' &= \frac{1}{24} m_i^- m_i^+ (m_i^- \ddot{m}_i^- - m_i^+ \ddot{m}_i^+) \end{aligned}$$

We introduce a new pair of variables (ρ, \mathcal{J}) on the lower singular strips, which is the counterpart of (τ, \mathcal{I}) as follows

$$\rho = \begin{cases} J(\zeta - \zeta_1^*) & \text{on } R_1^- \\ J(\zeta - \zeta_2^*) & \text{on } R_2^- \end{cases}, \quad \mathcal{J} = \frac{J}{\mathcal{M}_*} \text{ on } R_1^-, R_2^-$$

Proposition 4.4 (Lower-Lower). *Suppose that $(\rho_1, \mathcal{J}_1) \in R_1^-$, and $\mathcal{J}_1 > V_*$, and that*

$$f(t_2^*-) - f(t_2^*) \lesssim -m_2^- \{\mathcal{M}_* \mathcal{J}_1 (\zeta_2^* - \zeta_1^*) - \rho_1\}_2 \lesssim f(t_2^*-) + f(t_2^*+).$$

Then the Poincaré map $P_{LL}^{12} : R_1^- \rightarrow R_2^-$ is given by

$$(\bar{\rho}_2, \bar{\mathcal{J}}_2) = G_{LL}^{12}(\rho_1, \mathcal{J}_1) + H_{LL}^{12}(\rho_1, \mathcal{J}_1) + \mathcal{O}(\mathcal{J}_1^{-2})$$

where

$$G_{LL}^{12}(\rho_1, \mathcal{J}_1) = \left(-\frac{m_2^-}{m_2^+} \{\mathcal{M}_* \mathcal{J}_1 (\zeta_2^* - \zeta_1^*) - \rho_1\}_2 + 1 + \frac{m_2^-}{m_2^+}, \frac{m_2^-}{m_2^+} \mathcal{J}_1 + \Upsilon_2(\bar{\rho}_2 - 1) \right)$$

and

$$H_{LL}^{12}(\rho_1, \mathcal{J}_1) = (0, \Upsilon_2'(\bar{\rho}_2 - 1)^2 / \mathcal{J}_1 + \Upsilon_2'' / \mathcal{J}_1).$$

Similarly, suppose that $(\rho_2, \mathcal{J}_2) \in R_2^-$ and $\mathcal{J}_2 > V_*$, and that

$$f(t_1^*-) - f(t_1^*) \lesssim -m_1^- \{\mathcal{M}_* \mathcal{J}_2 (2 + \zeta_1^* - \zeta_2^*) - \rho_2\}_2 \lesssim f(t_1^*-) + f(t_1^*+).$$

Then the Poincaré map $P_{LL}^{21} : R_2^- \rightarrow R_1^-$ is given by

$$(\bar{\rho}_1, \bar{\mathcal{J}}_1) = G_{LL}^{21}(\rho_2, \mathcal{J}_2) + H_{LL}^{21}(\rho_2, \mathcal{J}_2) + \mathcal{O}(\mathcal{J}_2^{-2})$$

where

$$G_{LL}^{21}(\rho_2, \mathcal{J}_2) = \left(-\frac{m_1^-}{m_1^+} \{\mathcal{M}_* \mathcal{J}_2 (2 + \zeta_1^* - \zeta_2^*) - \rho_2\}_2 + 1 + \frac{m_1^-}{m_1^+}, \frac{m_1^-}{m_1^+} \mathcal{J}_2 + \Upsilon_1(\bar{\rho}_1 - 1) \right),$$

$$H_{LL}^{21}(\rho_2, \mathcal{J}_2) = (0, \Upsilon_1'(\bar{\rho}_1 - 1)^2 / \mathcal{J}_2 + \Upsilon_1'' / \mathcal{J}_2),$$

and $m_i^\pm = m(t_i^* \pm)$.

4.2.3. The Upper-Lower Chamber Case. Now we suppose that $(\tilde{t}, \tilde{v}) \in \tilde{R}$ and that the ball is in the upper chamber. Also we assume that the next wall is above the previous one when the ball passes through the singularity at $t = t_*$: $f(t_*-) < f(t_*+)$. Let $(\bar{t}, \bar{v}) = F(\tilde{t}, \tilde{v})$.

If $v(t_* - t) > 2 - f(t) - f(t_*+)$, then the ball collides with the ceiling and then enters the lower chamber (c.f. Figure 4 on the left).

Rather than resorting to the detailed computation as we have done in the constant chamber cases, we insert an imaginary stationary slit, whose length is negligible, at the height $f_* = 1 - \tilde{v}(t_* - \tilde{t}) + l(\tilde{t})$, so that the two consecutive collisions at the moving slits are concatenated

by two fictional collisions at the imaginary wall, to which the Upper-Upper and Lower-Lower formulas readily apply.

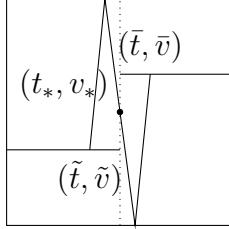


FIGURE 7. The Imaginary Stationary Wall

More precisely, as the ball leaves the previous slit at time \tilde{t} with velocity \tilde{v} , it collides against the imaginary tiny slit at time t_* and the outgoing velocity is still $v_* = \tilde{v}$ as the slit is stationary. Meanwhile we also imagine that the ball leaves from below the fictional slit at time t_* with velocity $v_* = -\tilde{v}$ (with an abuse of notation), then it collides at the next moving slit at time \bar{t} with outgoing velocity \bar{v} .

Let us denote $I_* = I(t_*, v_*)$, etc. We will need the following constants

$$\begin{aligned}\kappa_{Ii} &= \frac{1}{2}m_+(\dot{m}_+ - m_+\dot{l}_-/l_-) \\ \kappa'_{Ii} &= \frac{1}{2}m_+\dot{l}_-/l_- \\ \kappa''_{Ii} &= \frac{1}{8}m_+\ddot{l}_-(1 - \frac{1}{3}l_-^2) \\ \kappa'''_{Ii} &= \frac{1}{4}m_+^2(\ddot{l}_- + \frac{1}{6}l_-\ddot{m}_+) \\ \kappa''''_{Ii} &= \frac{1}{8}m_+^3\ddot{l}_- \\ \kappa''''_{Ii} &= \frac{1}{8}m_+^2\ddot{m}_+l_-\end{aligned}$$

where i indicates that $l(t)$ and $m(t)$ are evaluated at $t = t_i^*$ ($i = 1, 2$). Then the dynamics between the singular strips is captured by the following formula:

Proposition 4.5 (Upper-Lower I). *Assume that $(\tau_1, \mathcal{I}_1) \in R_1^+$ with $\mathcal{I}_1 > V_*$ and that*

$$l_2^- \{\mathcal{L}_* \mathcal{I}_1(\theta_2^* - \theta_1^*) - \tau_1\}_2 \gtrsim 2 - f(t_2^+) - f(t_2^*-).$$

Then the Poincaré map $P_{ULI}^{12} : R_1^+ \rightarrow R_2^-$ is given by

$$(\bar{\rho}_2, \bar{\mathcal{J}}_2) = G_{ULI}^{12}(\tau_1, \mathcal{I}_1) + H_{ULI}^{12}(\tau_1, \mathcal{I}_1) + \mathcal{O}(\mathcal{I}_1^{-2})$$

where

$$G_{ULI}^{12}(\tau_1, \mathcal{I}_1) = \left(\frac{l_2^-}{m_2^+} \{ \mathcal{L}_* \mathcal{I}_1 (\theta_2^* - \theta_1^*) - \tau_1 \}_2 + \frac{m_2^+ - l_2^- - 1}{m_2^+}, \right. \\ \left. - \frac{m_2^+}{l_2^-} \mathcal{I}_1 + \kappa_{I_2} (\bar{\rho}_2 - 1) - \kappa'_{I_2} \right)$$

and

$$H_{ULI}^{12}(\tau_1, \mathcal{I}_1) = \left(0, \frac{\kappa''_{I_2}}{\mathcal{I}_1} + \kappa'''_{I_2} \frac{\bar{\rho}_2 - 1}{\mathcal{I}_1} + \kappa''''_{I_2} \frac{(\bar{\rho}_2 - 1)^2}{\mathcal{I}_1} - \kappa''''_{I_2} \frac{(\bar{\rho}_2 - 1)^3}{\mathcal{I}_1} \right).$$

Similarly, assume that $(\tau_2, \mathcal{I}_2) \in R_2^+$ with $\mathcal{I}_2 > V_*$ and that

$$l_1^- \{ \mathcal{L}_* \mathcal{I}_2 (2 + \theta_1^* - \theta_2^*) - \tau_2 \}_2 \gtrsim 2 - f(t_1^+) - f(t_1^* -).$$

Then the Poincaré map $P_{ULI}^{21} : R_2^+ \rightarrow R_1^-$ is given by

$$(\bar{\rho}_1, \bar{\mathcal{J}}_1) = G_{ULI}^{21}(\tau_2, \mathcal{I}_2) + H_{ULI}^{21}(\tau_2, \mathcal{I}_2) + \mathcal{O}(\mathcal{I}_2^{-2})$$

where

$$G_{ULI}^{21}(\tau_2, \mathcal{I}_2) = \left(\frac{l_1^-}{m_1^+} \{ \mathcal{L}_* \mathcal{I}_2 (2 + \theta_1^* - \theta_2^*) - \tau_2 \}_2 + \frac{m_1^+ - l_1^- - 1}{m_1^+}, \right. \\ \left. - \frac{m_1^+}{l_1^-} \mathcal{I}_2 + \kappa_{I_1} (\bar{\rho}_1 - 1) - \kappa'_{I_1} \right)$$

and

$$H_{ULI}^{21}(\tau_2, \mathcal{I}_2) = \left(0, \frac{\kappa''_{I_1}}{\mathcal{I}_2} + \kappa'''_{I_1} \frac{\bar{\rho}_1 - 1}{\mathcal{I}_2} + \kappa''''_{I_1} \frac{(\bar{\rho}_1 - 1)^2}{\mathcal{I}_2} - \kappa''''_{I_1} \frac{(\bar{\rho}_1 - 1)^3}{\mathcal{I}_2} \right).$$

Proof. We present the proof of P_{ULI}^{12} . The formula for P_{ULI}^{21} can be obtained similarly. We suppress the sub/superscripts whenever they are clear from the context.

We imagine that the ball collides at the fictional stationary wall at time t_* with outgoing velocity $v_* = \tilde{v}$. Then $l_* = 1 - f_* = \tilde{v}(t_* - \tilde{t}) - l(\tilde{t})$ and we have

$$I_* = \frac{L_*}{2} l_* \tilde{v}, \quad \tau_* = 0.$$

From the Upper-Upper formula,

$$\tau_* = \frac{l_-}{l_*} \tilde{I}(\tilde{\theta} - \theta_2^*) + 1 + \frac{l_-}{l_*} + \mathcal{O}(v^{-2}) \\ I_* = \frac{l_*}{l_-} \tilde{I} + \frac{L_* l_*^2}{2l_-} \dot{l}_- - \frac{L_*^2 l_*^3 \ddot{l}_-}{8\tilde{I}} + \frac{L_*^2 l_*^2 l_- \ddot{l}_-}{24\tilde{I}} + \mathcal{O}(v^{-2}).$$

Now we imagine that the ball leaves from below the fictional stationary wall at time t_* with outgoing velocity $v_* = -\tilde{v}$ (with an abuse of notation). Then $m_* = -m(\bar{t}) - v(\bar{t} - t_*)$ and we have

$$J_* = -\frac{M_*}{2}m_*\tilde{v}, \quad \rho_* = 0.$$

From the Lower-Lower formula,

$$\bar{\rho} = 1 + \frac{m_*}{m_+} + \mathcal{O}(v^{-2})$$

$$\bar{J} = \frac{m_+}{m_*}J_* + \frac{M_*}{2}m_+\dot{m}_+(\bar{\rho}-1) + \frac{M_*^2}{8J_*}m_+^2m_*\ddot{m}_+(\bar{\rho}-1)^2 - \frac{M_*^2}{24J_*}m_+^2m_*\ddot{m}_+ + \mathcal{O}(v^{-2}).$$

We observe that

$$\begin{aligned} l_* &= v(t_* - \tilde{t}) - l(\tilde{t}) \\ &= v(t_* - \tilde{t}) - l_- - \dot{l}_-(\tilde{t} - t_*) + \mathcal{O}(v^{-2}) \\ &= -(\tilde{v} + \dot{l}_-)(t_* - \tilde{t}) - l_- + \mathcal{O}(v^{-2}) \\ &= -l_- \tilde{I}(\tilde{\theta} - \theta_2^*) - l_- + \mathcal{O}(v^{-2}) \end{aligned}$$

and that

$$\begin{aligned} m_* &= -m(\bar{t}) - v(\bar{t} - t_*) \\ &= -m_+ - \dot{m}_+(\bar{t} - t_*) + (\bar{v} + 2\dot{m}_+)(\bar{t} - t_*) + \mathcal{O}(v^{-2}) \\ &= -m_+ + (\bar{v} + \dot{m}_+)(\bar{t} - t_*) + \mathcal{O}(v^{-2}) \\ &= -m_+ + m_+\bar{\rho} + \mathcal{O}(v^{-2}) \end{aligned}$$

Since $m_* = l_* - 1$,

$$\bar{\rho} = -\frac{l_-}{m_+} \tilde{I}(\tilde{\theta} - \theta_2^*) + \frac{m_+ - l_- - 1}{m_+} + \mathcal{O}(v^{-2}).$$

Finally the relation between I_* and J_* , together with Lemma 4.1, produces the formula for \bar{J} . \square

If $v(t_* - t) < f(t_+,) - f(t)$, then the ball enters the lower chamber immediately after it leaves the previous slit (c.f. Figure 3 on the right). The imaginary wall trick no longer applies, so we have to return to the direct computation.

We will need the following constants

$$\begin{aligned}\kappa''_{\text{II}i} &= \frac{1}{4}m_+^2\ddot{l}_- \\ \kappa'''_{\text{II}i} &= \frac{1}{8}m_+^2(l_-\ddot{m}_+ - m_+\ddot{l}_-) \\ \kappa''''_{\text{II}i} &= \frac{1}{24}m_+l_-(l_-^2\ddot{l}_- - l_-m_+\ddot{m}_+ - 3\ddot{l}_-)\end{aligned}$$

where i indicates that $l(t)$ and $m(t)$ are evaluated at $t = t_i^*$ ($i = 1, 2$).

Proposition 4.6 (Upper-Lower II). *Assume that $(\tau_1, \mathcal{I}_1) \in R_1^+$ with $\mathcal{I}_1 > V_*$ and that*

$$f(t_2^+) - f(t_2^*) \gtrsim l_2^- \{\mathcal{L}_* \mathcal{I}_1 (\theta_2^* - \theta_1^*) - \tau_1\}_2.$$

Then the Poincaré map $P_{UL\text{II}}^{12} : R_1^+ \rightarrow R_2^-$ is given by

$$(\bar{\rho}_2, \bar{\mathcal{J}}_2) = G_{UL\text{II}}^{12}(\tau_1, \mathcal{I}_1) + H_{UL\text{II}}^{12}(\tau_1, \mathcal{I}_1) + \mathcal{O}(\mathcal{I}_1^{-2})$$

where

$$\begin{aligned}G_{UL\text{II}}^{12}(\tau_1, \mathcal{I}_1) &= \left(\frac{l_2^-}{m_2^+} \{\mathcal{L}_* \mathcal{I}_1 (\theta_2^* - \theta_1^*) - \tau_1\}_2 + \frac{m_2^+ - l_2^- + 1}{m_2^+}, \right. \\ &\quad \left. - \frac{m_2^+}{l_2^-} \mathcal{I}_1 + \kappa_{\text{I}2}(\bar{\rho}_2 - 1) + \kappa'_{\text{I}2} \right)\end{aligned}$$

and

$$H_{UL\text{II}}^{12}(\tau_1, \mathcal{I}_1) = \left(0, -\kappa''_{\text{II}2} \frac{\bar{\rho}_2 - 1}{\mathcal{I}_1} - \kappa'''_{\text{II}2} \frac{(\bar{\rho}_2 - 1)^2}{\mathcal{I}_1} - \frac{\kappa''''_{\text{II}2}}{\mathcal{I}_1} \right).$$

Similarly, assume that $(\tau_2, \mathcal{I}_2) \in R_2^+$ with $\mathcal{I}_2 > V_*$ and that

$$f(t_1^+) - f(t_1^*) \gtrsim l_1^- \{\mathcal{L}_* \mathcal{I}_2 (2 + \theta_1^* - \theta_2^*) - \tau_2\}_2.$$

Then the Poincaré map $P_{UL\text{II}}^{21} : R_2^+ \rightarrow R_1^-$ is given by

$$(\bar{\rho}_1, \bar{\mathcal{J}}_1) = G_{UL\text{II}}^{21}(\tau_2, \mathcal{I}_2) + H_{UL\text{II}}^{21}(\tau_2, \mathcal{I}_2) + \mathcal{O}(\mathcal{I}_2^{-2})$$

where

$$\begin{aligned}G_{UL\text{II}}^{21}(\tau_2, \mathcal{I}_2) &= \left(\frac{l_1^-}{m_1^+} \{\mathcal{L}_* \mathcal{I}_2 (2 + \theta_1^* - \theta_2^*) - \tau_2\}_2 + \frac{m_1^+ - l_1^- + 1}{m_1^+}, \right. \\ &\quad \left. - \frac{m_1^+}{l_1^-} \mathcal{I}_2 + \kappa_{\text{I}1}(\bar{\rho}_1 - 1) + \kappa'_{\text{I}1} \right)\end{aligned}$$

and

$$H_{UL\text{II}}^{21}(\tau_2, \mathcal{I}_2) = \left(0, -\kappa''_{\text{II}1} \frac{\bar{\rho}_1 - 1}{\mathcal{I}_2} - \kappa'''_{\text{II}1} \frac{(\bar{\rho}_1 - 1)^2}{\mathcal{I}_2} - \frac{\kappa''''_{\text{II}1}}{\mathcal{I}_2} \right).$$

Proof. Again we only prove the formula for P_{ULII}^{12} . We have from Equation (5) that

$$\begin{aligned}
v(\bar{t} - \tilde{t}) &= f(\bar{t}) - f(\tilde{t}) \\
\implies \tilde{v}((\bar{t} - t_*) - (\tilde{t} - t_*)) &= -m(\bar{t}) + l(\tilde{t}) - 1 \\
\implies m_+ - (\bar{v} + \dot{m}_+)(\bar{t} - t_*) &= (\tilde{v} + \dot{l}_-)(\tilde{t} - t_*) + l_- - 1 + \mathcal{O}(v^{-2}) \\
\implies m_+ - m_+\bar{\rho} &= l_- \tilde{I}(\tilde{\theta} - \theta_2^*) + l_- - 1 + \mathcal{O}(v^{-2}) \\
\implies \bar{\rho} &= -\frac{l_-}{m_+} \tilde{I}(\tilde{\theta} - \theta_2^*) + \frac{m_+ - l_- + 1}{m_+} + \mathcal{O}(v^{-2})
\end{aligned}$$

The computation is similar to that in the proof of Proposition 4.3. So we just list the key steps.

We observe that

$$\begin{aligned}
2\mathcal{M}_*^{-1} \bar{J} &= \bar{m}\bar{v} + \bar{m}\dot{\bar{m}} + \frac{\bar{m}^2 \ddot{\bar{m}}}{3\bar{v}} \\
&= m_+\bar{v} + m_+\dot{m}_+ + m_+\dot{m}_+\bar{\rho} + m_+\ddot{m}_+(\bar{t} - t_*) + \frac{m_+^2 \ddot{m}_+}{3\bar{v}} \\
&\quad + \frac{\ddot{m}_+}{2}(\bar{t} - t_*)^2 \bar{v} + \mathcal{O}(v^{-2})
\end{aligned}$$

and that

$$\begin{aligned}
2\mathcal{L}_*^{-1} \tilde{I} &= \tilde{l}\tilde{v} + \tilde{l}\dot{\tilde{l}} + \frac{\tilde{l}^2 \ddot{\tilde{l}}}{3\tilde{v}} \\
&= l_-\tilde{v} + l_-\dot{l}_- + l_-\dot{l}_- \tilde{I}(\tilde{\theta} - \theta_2^*) + l_-\ddot{l}_-(\tilde{t} - t_*) + \frac{l_-^2 \ddot{l}_-}{3\tilde{v}} \\
&\quad + \frac{\ddot{l}_-}{2}(\tilde{t} - t_*)^2 \tilde{v} + \mathcal{O}(v^{-2}).
\end{aligned}$$

We also note from Equation (5) that

$$\tilde{v} = -\bar{v} - 2\dot{m}_+ - 2\ddot{m}_+(\bar{t} - t_*) + \mathcal{O}(v^{-2})$$

and that

$$\begin{aligned}
\bar{t} - \tilde{t} &= \frac{f(\bar{t}) - f(\tilde{t})}{\tilde{v}} = \frac{-m(\bar{t}) + l(\tilde{t}) - 1}{\tilde{v}} \\
&= \frac{-m_+ + l_- - 1}{\tilde{v}} + (-\dot{m}_+ + \dot{l}_-) \frac{\bar{t} - t_*}{\tilde{v}} - \dot{l}_- \frac{\bar{t} - \tilde{t}}{\tilde{v}} + \mathcal{O}(v^{-3}) \\
&= \frac{-m_+ + l_- - 1}{\tilde{v}} + (-\dot{m}_+ + \dot{l}_-) \frac{\bar{t} - t_*}{\tilde{v}} + \dot{l}_- \frac{m_+ - l_- + 1}{\tilde{v}^2} + \mathcal{O}(v^{-3}).
\end{aligned}$$

Therefore

$$\begin{aligned} 2\mathcal{L}_*^{-1}\tilde{I} &= -l_-\bar{v} - 2l_-\dot{m}_+ + m_+\dot{l}_- + m_+\dot{l}_-\bar{\rho} + \dot{l}_- \\ &\quad + (m_+\ddot{l}_- - 2l_-\ddot{m}_+ + \ddot{l}_-)(\bar{t} - t_*) - \frac{\ddot{l}_-}{2}(\bar{t} - t_*)^2\bar{v} \\ &\quad - \frac{\ddot{l}_-}{2\bar{v}} \left((m_+ + 1)^2 - \frac{l_-^2}{3} \right) + \mathcal{O}(v^{-2}) \end{aligned}$$

hence

$$\begin{aligned} \frac{2l_-}{\mathcal{M}_*}\bar{J} + \frac{2m_+}{\mathcal{L}_*}\tilde{I} &= m_+\dot{l}_- + m_+(l_-\dot{m}_+ - m_+\dot{l}_-)(\bar{\rho} - 1) - \frac{1}{2}\mathcal{L}_*l_-m_+^2\ddot{l}_-\frac{\bar{\rho} - 1}{I} \\ &\quad - \frac{1}{4}\mathcal{L}_*l_-m_+^2(l_-\ddot{m}_+ - m_+\ddot{l}_-)\frac{(\bar{\rho} - 1)^2}{I} \\ &\quad - \frac{1}{12I}\mathcal{L}_*l_-m_+(l_-^2\ddot{l}_- - l_-m_+\ddot{m}_+ - 3\ddot{l}_-) + \mathcal{O}(v^{-2}) \end{aligned}$$

which produces the desired formula together with Lemma 4.1. \square

4.2.4. *The Lower-Upper Chamber Case.* Finally we suppose that $(\tilde{t}, \tilde{v}) \in \tilde{R}$ and that the ball is in the lower chamber. Also we assume that the next wall is below the previous one when the ball passes through the singularity at $t = t_*$: $f(t_*-) > f(t_*+)$. Again let $(\bar{t}, \bar{v}) = F(\tilde{t}, \tilde{v})$.

If $-v(t_* - t) > f(t) + f(t_*-)$, then the ball collides with the floor and enters the upper chamber (c.f. Figure 4 on the left).

The imaginary stationary wall trick also applies in this case, which produces a desired formula with the following constants

$$\begin{aligned} \chi_{Ii} &= \frac{1}{2}l_+(\dot{l}_+ - l_+\dot{m}_-/m_-) \\ \chi'_{Ii} &= \frac{1}{2}l_+\dot{m}_-/m_- \\ \chi''_{Ii} &= \frac{1}{8}l_+\ddot{m}_-(1 - \frac{1}{3}m_-^2) \\ \chi'''_{Ii} &= \frac{1}{4}l_+^2(\frac{1}{6}m_-\ddot{l}_+ - \ddot{m}_-) \\ \chi''''_{Ii} &= \frac{1}{8}l_+^3\ddot{m}_- \\ \chi''''_{Ii} &= \frac{1}{8}l_+^2\ddot{l}_+m_- \end{aligned}$$

where i indicates that $l(t)$ and $m(t)$ are evaluated at $t = t_i^*$ ($i = 1, 2$).

Proposition 4.7 (Lower-Upper I). *Assume that $(\rho_1, \mathcal{J}_1) \in R_1^-$ with $\mathcal{J}_1 > V_*$ and that $-m_2^- \{\mathcal{M}_* \mathcal{J}_1 (\zeta_2^* - \zeta_1^*) - \rho_1\}_2 \gtrsim f(t_2^*-) + f(t_2^*+)$. Then the Poincaré map $P_{LUI}^{12} : R_1^- \rightarrow R_2^+$ is given by*

$$(\bar{\tau}_2, \bar{\mathcal{I}}_2) = G_{LUI}^{12}(\rho_1, \mathcal{J}_1) + H_{LUI}^{12}(\rho_1, \mathcal{J}_1) + \mathcal{O}(\mathcal{J}_1^{-2})$$

where

$$G_{LUI}^{12}(\rho_1, \mathcal{J}_1) = \left(\frac{m_2^-}{l_2^+} \{\mathcal{M}_* \mathcal{J}_1 (\zeta_2^* - \zeta_1^*) - \rho_1\}_2 + \frac{l_2^+ - m_2^- + 1}{l_2^+}, \right. \\ \left. - \frac{l_2^+}{m_2} \mathcal{J}_1 + \chi_{I2}(\bar{\tau}_2 - 1) + \chi'_{I2} \right)$$

and

$$H_{LUI}^{12}(\rho_1, \mathcal{J}_1) = \left(0, \frac{\chi''_{I2}}{\mathcal{J}_1} + \chi'''_{I2} \frac{\bar{\tau}_2 - 1}{\mathcal{J}_1} + \chi''''_{I2} \frac{(\bar{\tau}_2 - 1)^2}{\mathcal{J}_1} - \chi''''_{I2} \frac{(\bar{\tau}_2 - 1)^3}{\mathcal{J}_1} \right).$$

Similarly, assume that $(\rho_2, \mathcal{J}_2) \in R_2^-$ with $\mathcal{J}_2 > V_*$ and that

$$-m_1^- \{\mathcal{M}_* \mathcal{J}_2 (2 + \zeta_1^* - \zeta_2^*) - \rho_2\}_2 \gtrsim f(t_1^*-) + f(t_1^*+).$$

Then the Poincaré map $P_{LUI}^{21} : R_2^- \rightarrow R_1^+$ is given by

$$(\bar{\tau}_1, \bar{\mathcal{I}}_1) = G_{LUI}^{21}(\rho_2, \mathcal{J}_2) + H_{LUI}^{21}(\rho_2, \mathcal{J}_2) + \mathcal{O}(\mathcal{J}_2^{-2})$$

where

$$G_{LUI}^{21}(\rho_2, \mathcal{J}_2) = \left(\frac{m_1^-}{l_1^+} \{\mathcal{M}_* \mathcal{J}_2 (2 + \zeta_1^* - \zeta_2^*) - \rho_2\}_2 + \frac{l_1^+ - m_1^- + 1}{l_1^+}, \right. \\ \left. \frac{l_1^+}{m_1} \mathcal{J}_2 + \chi_{I1}(\bar{\tau}_1 - 1) + \chi'_{I1} \right)$$

and

$$H_{LUI}^{21}(\rho_2, \mathcal{J}_2) = \left(0, \frac{\chi''_{I1}}{\mathcal{J}_2} + \chi'''_{I1} \frac{\bar{\tau}_1 - 1}{\mathcal{J}_2} + \chi''''_{I1} \frac{(\bar{\tau}_1 - 1)^2}{\mathcal{J}_2} - \chi''''_{I1} \frac{(\bar{\tau}_1 - 1)^3}{\mathcal{J}_2} \right).$$

Next, if $-v(t_* - t) < f(t) - f(t_*-)$, then the ball enters the lower chamber immediately after it leaves the previous slit (c.f. Figure 5 on the right).

The computation as we have performed for Proposition 4.6 can be reproduced here to present the formula in this case, the proof of which we ergo omit. We will need the following constants

$$\chi''_{III} = \frac{1}{4} l_+^2 \ddot{m}_- \\ \chi'''_{III} = \frac{1}{8} l_+^2 (m_- \ddot{l}_+ - l_+ \ddot{m}_-) \\ \chi''''_{III} = \frac{1}{24} l_+ m_- (m_-^2 \ddot{m}_- - m_- l_+ \ddot{l}_+ - 3 \ddot{m}_-)$$

where i indicates that $l(t)$ and $m(t)$ are evaluated at $t = t_i^*$ ($i = 1, 2$).

Proposition 4.8 (Lower-Upper II). *Assume that $(\rho_1, \mathcal{J}_1) \in R_1^-$ with $\mathcal{J}_1 > V_*$ and that $f(t_2^*-) - f(t_2^*+) \gtrsim -m_2^- \{\mathcal{M}_* \mathcal{J}_1 (\zeta_2^* - \zeta_1^*) - \rho_1\}_2$. Then the Poincaré map $P_{LU\text{II}}^{12} : R_1^- \rightarrow R_2^+$ is given by*

$$(\bar{\tau}_2, \bar{\mathcal{L}}_2) = G_{LU\text{II}}^{12}(\rho_1, \mathcal{J}_1) + H_{LU\text{II}}^{12}(\rho_1, \mathcal{J}_1) + \mathcal{O}(\mathcal{J}_1^{-2})$$

where

$$G_{LU\text{II}}^{12}(\rho_1, \mathcal{J}_1) = \left(\frac{m_2^-}{l_2^+} \{\mathcal{M}_* \mathcal{J}_1 (\zeta_2^* - \zeta_1^*) - \rho_1\}_2 + \frac{l_2^+ - m_2^- - 1}{l_2^+}, \right. \\ \left. - \frac{l_2^+}{m_2^-} \mathcal{J}_1 + \chi_{I2}(\bar{\tau}_2 - 1) - \chi'_{I2} \right)$$

and

$$H_{LU\text{II}}^{12}(\rho_1, \mathcal{J}_1) = \left(0, \chi''_{\text{II}2} \frac{\bar{\tau}_2 - 1}{\mathcal{J}_1} - \chi'''_{\text{II}2} \frac{(\bar{\tau}_2 - 1)^2}{\mathcal{J}_1} - \frac{\chi''''_{\text{II}2}}{\mathcal{J}_1} \right).$$

Similarly, assume that $(\rho_2, \mathcal{J}_2) \in R_2^-$ with $\mathcal{J}_2 > V_*$ and that

$$f(t_1^*-) - f(t_1^*+) \gtrsim -m_1^- \{\mathcal{M}_* \mathcal{J}_2 (2 + \zeta_1^* - \zeta_2^*) - \rho_2\}_2.$$

Then the Poincaré map $P_{LU\text{II}}^{21} : R_2^- \rightarrow R_1^+$ is given by

$$(\bar{\tau}_1, \bar{\mathcal{L}}_1) = G_{LU\text{II}}^{21}(\rho_2, \mathcal{J}_2) + H_{LU\text{II}}^{21}(\rho_2, \mathcal{J}_2) + \mathcal{O}(\mathcal{J}_2^{-2})$$

where

$$G_{LU\text{II}}^{21}(\rho_2, \mathcal{J}_2) = \left(\frac{m_1^-}{l_1^+} \{\mathcal{J}_2 (2 + \zeta_1^* - \zeta_2^*) - \rho_2\}_2 + \frac{l_1^+ - m_1^- - 1}{l_1^+}, \right. \\ \left. - \frac{l_1^+}{m_1^-} \mathcal{J}_2 + \chi_{\text{II}}(\bar{\tau}_1 - 1) - \chi'_{\text{II}} \right)$$

and

$$H_{LU\text{II}}^{21}(\rho_2, \mathcal{J}_2) = \left(0, \chi''_{\text{II}1} \frac{\bar{\tau}_1 - 1}{\mathcal{J}_2} - \chi'''_{\text{II}1} \frac{(\bar{\tau}_1 - 1)^2}{\mathcal{J}_2} - \frac{\chi''''_{\text{II}1}}{\mathcal{J}_2} \right).$$

5. TRAPPING REGIONS

In this section, we present the proof of Theorem 1. The assumptions in the theorem lead to the creation of a trapping region where the ball gains energy exponentially fast.

Proof. We choose $V_* \gg 1$ so that the normal forms in Section 4 hold for $|v| > V_*$. There are two cases.

(i) Suppose that $f_L(t_1^*) < f_R(t_1^*)$ and $f_L(t_2^*) > f_R(t_2^*)$. The relative positions of the two slits at two critical jumps trap the ball forever in

the lower region once it enters. Henceforth Proposition 4.4 predicts the change of energy after one period in the lower chamber to be

$$\bar{\mathcal{J}} = \frac{m_1^+ m_2^+}{m_1^- m_2^-} \mathcal{J} + \mathcal{O}(1)$$

Furthermore, the relative positions of the slits at two critical times guarantee that $m(t_1^+) < m(t_1^* -) < 0$, $m(t_2^+) < m(t_2^* -) < 0$, so the energy of the ball grows exponentially fast at rate $\frac{m_1^+ m_2^+}{m_1^- m_2^-} > 1$ in the lower chamber.

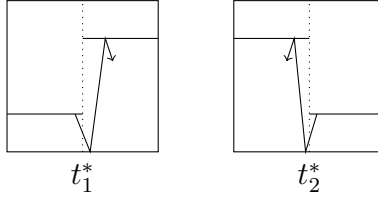


FIGURE 8. The Trapping Lower Chamber

If the ball starts from the lower chamber with $v_0 < -V_*$, it enjoys exponential energy growth with time immediately.

If the ball starts from the upper chamber with $v_0 > V_*$, by Proposition 4.3 and the relative positions of the slits, its energy decreases at an exponential rate $\frac{t_1^+ t_2^+}{t_1^- t_2^-} < 1$ until it either enters the lower chamber or it enters the low energy region $|v| < V_*$ and the normal form no longer applies. For any $V > V_*$, we denote

$$\mathcal{U}_V = \{(t_0, v_0) : V < v_0 < V + 1, \limsup v_n < V_*\}$$

We claim that $\text{mes}(\mathcal{U}_V) = 0$. Otherwise we note that $\mathcal{U}_V \subseteq \{|v_n| < V + 1, \forall n > 0\}$, which is bounded and invariant. Hence, the Poincaré recurrence theorem implies that almost every point in \mathcal{U}_V would return infinitely often to energy level $|v_n| > V$, which is impossible as it would contradict the definition of \mathcal{U}_V . Our claim implies that almost all points in the energy shell $\mathcal{W}_V = \{V < v < V + 1\}$ eventually return to high energy level $|v_n| > V_*$, which is only made possible if the ball enters the lower chamber and the foregoing discussion ensures exponential energy growth afterwards.

(ii) Suppose that $f_L(t_1^*) > f_R(t_1^*)$ and $f_L(t_2^*) < f_R(t_2^*)$. Now the relative positions of the two slits at two critical jumps indicate that the upper region is trapping and then Proposition 4.3 guarantees an exponential

energy gain at rate $\frac{l_1^+ l_2^+}{l_1^- l_2^-} > 1$ in the upper chamber once the ball gets trapped. The rest of the analysis is similar to Case (i). \square

Example 5.1. In general it is not possible to improve the result that non-escaping orbits have finite measure to one with zero measure. For example, we start with $\tilde{f}_L(t) = \tilde{f}_R(t) = a \cos 4\pi t + 0.5$ for some small $a > 0$. We take $x_0 = 0, \lambda = 0.5$, so $t_1^* = 0.5, t_2^* = 1.5$. We consider a 4-periodic orbit \mathcal{P} starting at $t_0 = 0.25, v_0 = 2 + 4a$. Then

$$(t_1, v_1) = (0.75, 2+4a), \quad (t_2, v_2) = (1.25, 2+4a), \quad (t_3, v_3) = (1.75, 2+4a), \quad .$$

We can slightly modify \tilde{f}_L near t_1^*, t_2^* in such a way that

$$f_L(0.5) > f_R(0.5), \quad f_L(1.5) < f_R(1.5)$$

so that the upper chamber is trapping and that the periodic orbit \mathcal{P} does not see this modification. Observe that \mathcal{P} is elliptic for all small a as the trace of the collision map F along \mathcal{P} is $tr(dF_{\mathcal{P}}) = 2 - \frac{8a\pi^2}{1+2a} \in (0, 2)$ for $0 < a < \frac{1}{4\pi^2 - 2}$. Now the matrix $dF_{\mathcal{P}}$ is conjugate to a rotation by $2\pi\alpha$ with $\cos 2\pi\alpha = 1 - \frac{4a\pi^2}{1+2a}$. We can easily choose a such that the rotation angle α is Diophantine, then Herman's Last Geometric Theorem guarantees the stability of the elliptic orbit \mathcal{P} , i.e. there exists an elliptic island of bounded trajectories around \mathcal{P} (c.f. [7, Theorem 4]).

Although the assumptions of Theorem 1 are compatible with existence of a positive measure set of bounded orbits, we can eliminate the possibility of oscillatory orbits. Recall that a (forward) oscillatory orbit is an orbit such that

$$\limsup_{t \rightarrow +\infty} |v(t)| = \infty \quad \text{and} \quad \liminf_{t \rightarrow +\infty} |v(t)| < \infty.$$

Corollary 5.2. *In presence of a trapping region oscillatory orbits do not exist.*

Proof. We may assume without loss of generality that the lower chamber is trapping. All the high energy orbits in the lower chamber gain energy exponentially immediately.

Now suppose that the ball is in the upper chamber and arrives at high energy level at some $v > V_*$, then it decelerates exponentially as observed in the proof of Theorem 1 until it hits the lower chambers or the normal form no longer applies. In either case, it either starts to accelerate exponentially or remains in the low energy region $|v| < V_*$ afterwards. \square

6. WAITING TIME FOR EXPONENTIAL ACCELERATION

In this section we show that in the presence of the trapping region, the majority of orbits with sufficiently high energy get trapped quickly under the hyperbolicity assumption. Throughout this section we assume without loss of generality that the lower chamber is trapping and $|Tr| > 2$. The quantity Tr is in fact the trace of the derivative of the linear map $G_U = G_{UU}^{21} \circ G_{UU}^{12}$ and the hyperbolicity assumption $|Tr| > 2$ indicates that G_U is hyperbolic.

6.1. Almost Sure Escape for the Limiting Map. We first restrict ourselves to the linear parts G_{UU} 's of the dynamics in Proposition 4.3, which approximates P_{UU} 's with an error of order $\mathcal{O}(I^{-1})$ when the velocity is large $v > V_*$.

We note that

$$\begin{aligned} (\bar{\tau}_2, \bar{I}_2) &= G_{UU}^{12}(\tau_1, I_1) \\ &= \left(-\frac{l_2^-}{l_2^+} \{ \mathcal{L}_* \mathcal{I}_1(\theta_2^* - \theta_1^*) - \tau_1 \}_2 + 1 + \frac{l_2^-}{l_2^+}, \frac{l_2^+}{l_2^-} \mathcal{I}_1 + \Delta_2(\bar{\tau}_2 - 1) \right) \end{aligned}$$

if $1 - \frac{l_2^+}{l_2^-} < \{ \mathcal{L}_* \mathcal{I}_1(\theta_2^* - \theta_1^*) - \tau_1 \}_2 < 1 + \frac{l_2^+}{l_2^-}$. The boundary lines

$$(9) \quad \{ \mathcal{L}_* \mathcal{I}_1(\theta_2^* - \theta_1^*) - \tau_1 \}_2 = 1 - \frac{l_2^+}{l_2^-}, \quad \{ \mathcal{L}_* \mathcal{I}_1(\theta_2^* - \theta_1^*) - \tau_1 \}_2 = 1 + \frac{l_2^+}{l_2^-}$$

cut out from R_1^+ a sequence of boxes

$$A_n = \left\{ 1 - \frac{l_2^+}{l_2^-} + 2n < \mathcal{L}_* \mathcal{I}_1(\theta_2^* - \theta_1^*) - \tau_1 < 1 + \frac{l_2^+}{l_2^-} + 2n \right\}$$

whose points will remain in the upper chamber under G_{UU}^{12} , while the other points will enter the lower chamber, when jumping from right to left at t_2^* .

We also observe that

$$\begin{aligned} (\bar{\tau}_1, \bar{I}_1) &= G_{UU}^{21}(\tau_2, I_2) \\ &= \left(-\frac{l_1^-}{l_1^+} \{ \mathcal{L}_* \mathcal{I}_2(2 + \theta_1^* - \theta_2^*) - \tau_2 \}_2 + 1 + \frac{l_1^-}{l_1^+}, \frac{l_1^+}{l_1^-} \mathcal{I}_2 + \Delta_1(\bar{\tau}_1 - 1) \right) \end{aligned}$$

if $1 - \frac{l_1^+}{l_1^-} < \{ \mathcal{L}_* \mathcal{I}_2(2 + \theta_1^* - \theta_2^*) - \tau_2 \}_2 < 1 + \frac{l_1^+}{l_1^-}$ and that the boundary lines

$$(10) \quad \{ \mathcal{L}_* \mathcal{I}_2(2 + \theta_1^* - \theta_2^*) - \tau_2 \}_2 = 1 - \frac{l_1^+}{l_1^-}, \quad \{ \mathcal{L}_* \mathcal{I}_2(2 + \theta_1^* - \theta_2^*) - \tau_2 \}_2 = 1 + \frac{l_1^+}{l_1^-}$$

cut out from R_2^+ another sequence of boxes

$$B_n = \left\{ 1 - \frac{l_1^+}{l_1^-} + 2n < \mathcal{L}_* \mathcal{I}_2(2 + \theta_1^* - \theta_2^*) - \tau_2 < 1 + \frac{l_1^+}{l_1^-} + 2n \right\}$$

whose points will remain in the upper chamber under G_{UU}^{21} , while the points outside will enter the lower chamber, when jumping from left to right at t_1^* .

We define $G_U = G_{UU}^{21} \circ G_{UU}^{12}$ on R_1^+ . Both G_{UU}^{12} and G_{UU}^{21} are piecewise affine maps, and the derivative of G_U part is a constant matrix $DG_U = DG_{UU}^{21} \cdot DG_{UU}^{12}$ where

$$DG_{UU}^{12} = \begin{pmatrix} \frac{l_2^-}{l_2^+} & -\frac{l_2^-}{l_2^+} \mathcal{L}_*(\theta_2^* - \theta_1^*) \\ \Delta_2 \frac{l_2^-}{l_2^+} & -\Delta_2 \frac{l_2^-}{l_2^+} \mathcal{L}_*(\theta_2^* - \theta_1^*) + \frac{l_2^+}{l_2^-} \end{pmatrix},$$

$$DG_{UU}^{21} = \begin{pmatrix} \frac{l_1^-}{l_1^+} & -\frac{l_1^-}{l_1^+} \mathcal{L}_*(2 + \theta_1^* - \theta_2^*) \\ \Delta_1 \frac{l_1^-}{l_1^+} & -\Delta_1 \frac{l_1^-}{l_1^+} \mathcal{L}_*(2 + \theta_1^* - \theta_2^*) + \frac{l_1^+}{l_1^-} \end{pmatrix}$$

Since $\det(DG_U) = 1$ and $|Tr(DG_U)| > 2$, it has unstable eigenvalue Λ_u with unstable eigenvector e_u , and stable eigenvalue Λ_s with stable eigenvector e_s .

We observe that each box A is foliated by unstable lines.

We say that an unstable line γ in a box A is *good* if it breaks after one period and at least two components remain in the upper chamber, otherwise we say it is *bad*.

A good line is good as a solid part of it enters the trapping region after one period under the linear map G_U :

Lemma 6.1. *Let γ be a good unstable line in some box A . Then the proportion of points on γ which remain in the upper chamber after one period is at most*

$$D = \frac{1 + 2\frac{l_1^+}{l_1^-}}{2 + \frac{l_1^+}{l_1^-}} < 1.$$

Proof. We first note that $G_{UU}^{12}(\gamma)$ remains a complete piece in R_2 as γ lies in A and that G_{UU}^{12} maps the boundaries of A into two vertical lines

$$G_{UU}^{12} \left(\{ \mathcal{L}_* \mathcal{I}_1(\theta_2^* - \theta_1^*) - \tau_1 \}_2 = 1 - \frac{l_2^+}{l_2^-} \right) \subseteq \{ \tau_2 = 2 \},$$

$$G_{UU}^{12} \left(\{ \mathcal{L}_* \mathcal{I}_1(\theta_2^* - \theta_1^*) - \tau_1 \}_2 = 1 + \frac{l_2^+}{l_2^-} \right) \subseteq \{ \tau_2 = 0 \}.$$

$G_{UU}^{12}(\gamma)$ has to stretch across at least two B -boxes if γ has at least two pieces remaining in the upper chamber after one period.

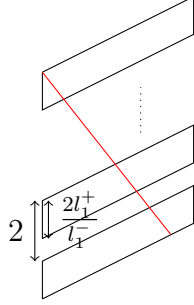


FIGURE 9. A good curve partly enters the trapping region

Suppose that $G_{UU}^{12}(\gamma)$ stretches across N B -boxes for some $N > 1$. It is easy to see that for a fixed N , the highest proportion of points staying in the upper chamber is achieved when $G_{UU}^{12}(\gamma)$ ends on the boundaries of the top and bottom boxes as shown in Figure 9. However the height of a B -box is equal to $2\frac{l_1^+}{l_1^+}$ (c.f. (10)) while the height of the fundamental domain is equal to 2 (c.f. Figure 9). This implies that in

the optimal situation $\frac{2(1-\frac{l_1^+}{l_1^+})(N-1)}{2N+2\frac{l_1^+}{l_1^+}}$ of the points on $G_{UU}^{12}(\gamma)$ land in the

lower chamber after jumping from left to right at t_1^* . This proportion is

larger than $\frac{(1-\frac{l_1^+}{l_1^+})(2-1)}{2+\frac{l_1^+}{l_1^+}}$ as it is an increasing function in N and $N \geq 2$.

Then the largest portion which remains in the upper chamber is given

by $D = \frac{1+2\frac{l_1^+}{l_1^+}}{2+\frac{l_1^+}{l_1^+}}$. Recall that the relative positions of two slits at t_1^* implies

that $\frac{l_1^+}{l_1^+} < 1$, so $D < 1$. □

Next we need to control the number of the short bad pieces as an unstable line breaks under the iterations of the linear map G_U .

Suppose γ is an unstable line in some box A . For $x \in \gamma$, we denote as $r_n(x)$ the distance from x_n to the nearest boundary of the component γ_n containing x_n . Employing the argument in Section 5 of [4] we obtain the following Growth Lemma.

Lemma 6.2 (Growth Lemma). *There exists a constant C^* s.t. for any small $\epsilon > 0$ and any $n \in \mathbb{N}$*

$$\text{mes}_\gamma\{x \in \gamma : r_n(x) < \epsilon\} \leq C^*\epsilon$$

Proof. Let $k_n(\delta)$ denote the max number of the pieces that an unstable line of length less than δ can be cut into. We define $k_n = \lim_{\delta \rightarrow 0} k_n(\delta)$. We claim that $k_n \leq 8n$. Indeed since the singularities of G_U^n are lines and there are at most $8n$ possibilities for slopes. Consequently, there exists δ_0 so small that $k_n(\delta) \leq 16n$ for any $\delta < \delta_0$. We choose n_0 such that $\frac{32n_0}{\Lambda_u^{n_0}} < 1$ and by replacing G_U with $G_U^{n_0}$ we can always assume $n_0 = 1$.

For inductive purposes we cut a long unstable line into pieces shorter than δ_0 and let $\bar{r}_n(x)$ denote the distance from x_n to the nearest real or artificial boundary of the component containing x_n . We note that by doing so we improve the estimate as $\bar{r}_n(x) \leq r_n(x)$ and it suffices to prove the statement for \bar{r}_n .

First we observe that

$$(11) \quad \text{mes}_\gamma \{ \bar{r}_0(x) < \epsilon \} \leq \frac{2L}{\delta_0} \epsilon.$$

$\bar{r}_{n+1}(x)$ is less than ϵ if x_{n+1} either passes a real or artificial singularity, where L is the unstable height of γ . The former is controlled by $2k_1(\delta_0)\text{mes}_\gamma \{ r_n < \frac{\epsilon}{\Lambda_u} \}$ while the latter by $2k_1(\delta_0)\frac{L}{\delta_0}\epsilon$. Therefore

$$\text{mes}_\gamma \{ \bar{r}_{n+1} < \epsilon \} \leq \frac{32}{\Lambda_u} \text{mes}_\gamma \{ r_n < \epsilon \} + 32 \frac{L}{\delta_0} \epsilon.$$

Thus by induction we conclude that

$$\text{mes}_\gamma \{ \bar{r}_n < \epsilon \} \leq \left(\frac{32}{\Lambda_u} \right)^n \text{mes}_\gamma \{ \bar{r}_0(x) < \epsilon \} + 32 \frac{L}{\delta_0} \epsilon \left(1 + \dots + \left(\frac{32}{\Lambda_u} \right)^{n-1} \right).$$

Since $\frac{32}{\Lambda_u} < 1$, (11) gives the desired growth control with

$$C^* = \left(\frac{32}{\Lambda_u} \right) \frac{2L}{\delta_0} + \frac{32L}{\delta_0(1 - \frac{32}{\Lambda_u})}. \quad \square$$

Finally we show that under the linear approximation map G_U almost every point will eventually escape to the trapping region:

Proposition 6.3. *In each box A , for any $\epsilon > 0$, there exists $N = N(\epsilon)$ such that all but an ϵ -measure set of points in A enter the lower chamber within N periods. In particular, almost every point will leave the upper chamber in the future.*

Proof. Fix $\epsilon > 0$. Choose k, l such that

$$D^k L < 0.5\epsilon \quad \text{and} \quad (kl + 1) \frac{C^* + L^2}{\Lambda_u^{l/2}} < 0.5\epsilon,$$

and take $N = kl + 1$.

We suppose that under the linear map G_U a point x on a unstable line γ stays in the upper chamber up to N periods.

If the trajectory of x lands on good lines more than k times in N periods, then Lemma 6.1 shows that for good lines the portion which remains in the upper chamber in the next period is at most D . Hence by induction we see that

$$\text{mes}_\gamma \{x \in \gamma : \{P_U^m x\}_{m=0}^N \text{ visits good lines more than } k \text{ times}\} < D^k L$$

If instead the trajectory of x visits good lines less than k times in N periods, then it has to visit consecutively l bad lines at least once in N periods.

Now suppose that the trajectory segment x_n, \dots, x_{n+l} land on bad lines $\gamma_n, \dots, \gamma_{n+l}$ for some $n < N$ and we denote as \mathcal{B}_n the set of all such $x \in \gamma$ that lands badly during n to $n+l$ periods. We subdivide \mathcal{B}_n into $\mathcal{B}_{n,L}$ and $\mathcal{B}_{n,S}$, where $\mathcal{B}_{n,L}$ collects points with $|\gamma_n| \geq \Lambda_u^{-l/2}$ and $\mathcal{B}_{n,S}$ collects points with $|\gamma_n| < \Lambda_u^{-l/2}$.

By Lemma 6.2, $|\mathcal{B}_{n,S}| \leq C^* \Lambda_u^{-l/2}$. On the other hand, it follows from uniform hyperbolicity that

$$\text{mes}_{\gamma_n} \{x_n \text{ returns badly for next } l \text{ periods}\} = \frac{|\gamma_{n+l}|}{\Lambda_u^l} \leq \frac{L}{\Lambda_u^l}.$$

Hence

$$|\mathcal{B}_{n,L}| \leq \frac{L}{\Lambda_u^l} \sum_{|\gamma_n| \geq \Lambda_u^{-l/2}} |G_U^{-n} \gamma_n| \leq \frac{L}{\Lambda_u^l} |\gamma| \leq \frac{L^2}{\Lambda_u^l}.$$

Combining the estimates on $\mathcal{B}_{n,L}$ and $\mathcal{B}_{n,S}$, we have

$$|\mathcal{B}_n| \leq \frac{C^*}{\Lambda_u^{l/2}} + \frac{L^2}{\Lambda_u^l} \leq \frac{C^* + L^2}{\Lambda_u^{l/2}}.$$

Consequently the set \mathcal{B} of points on γ which make l consecutive bad landings is controlled in size by

$$|\mathcal{B}| \leq (kl + 1) \frac{C^* + L^2}{\Lambda_u^{l/2}}.$$

Since a box A is foliated by unstable lines, we conclude by a disintegration of measure argument and our choice of k, l that under the linear map G_U the set of points in A which stay in the upper chamber for at least N periods has measure less than ϵ . \square

6.2. Quick Escape for the Actual Map. By Proposition 4.3, the fundamental domains of P_{UU} are $\mathcal{O}(\mathcal{I}^{-1})$ -deformation of the boxes A, B and $P_{UU} = G_{UU} + \mathcal{O}(\mathcal{I}^{-1})$.

Now we prove Theorem 2.

Proof of Theorem 2. Fix $\epsilon > 0$ and a box A with large energy $\tilde{\mathcal{I}}_0$ (to be specified later). By Proposition 6.3 we choose N such that in each A -box the points that remain in the upper chamber up to N periods under the linear approximation G_U take up a set of measure less than 0.5ϵ , i.e. we take $N = kl + 1$ where k, l are integers such that

$$(12) \quad k > \frac{\log(0.25\epsilon/L)}{\log D} \quad \text{and} \quad \frac{kl + 1}{\Lambda_u^{l/2}} < \frac{0.25\epsilon}{C^* + L^2}.$$

We shall show that the statement of Theorem 2 holds with some large $\tilde{\mathcal{I}}_0 = \tilde{\mathcal{I}}_0(\epsilon)$ and

$$(13) \quad T = 2N.$$

Let A_n^δ and B_n^δ denote the points in A_n and B_n which are closer than δ to the boundary,

$$\begin{aligned} \mathcal{A}^\delta &= \bigcup_n A_n^\delta, & \tilde{\mathcal{A}}^\delta &= \bigcup_n (A_n - \setminus A_n^\delta), \\ \mathcal{B}^\delta &= \bigcup_n B_n^\delta, & \tilde{\mathcal{B}}^\delta &= \bigcup_n (B_n - \setminus B_n^\delta). \end{aligned}$$

Choose $\delta < 0.5\epsilon$ so that the set of points in the box A which visit either \mathcal{A}^δ or \mathcal{B}^δ during the first N iterations is less than 0.5ϵ .

By Proposition 4.3, there is a constant C_1 such that if $P_{UU}^{12}(x) \in \tilde{\mathcal{B}}^{C_1/\mathcal{I}}$ and $P_{UU}^{21}(P_{UU}^{12}x) \in \tilde{\mathcal{A}}^{C_1/\mathcal{I}}$ then the orbit of x stays in the upper chamber for the next period and

$$|P_U(x) - G_U(x)| \leq \frac{C_1}{\mathcal{I}} \quad \text{where} \quad P_U = P_{UU}^{21} \circ P_{UU}^{12}.$$

Accordingly there is a constant C_2 such that if for some $n \leq N$

$$(14) \quad P_{UU}^{12}P_U^k(x) \in \tilde{\mathcal{B}}^{\frac{C_2\Lambda_u^N}{\mathcal{I}^*}}, \quad P_U^{k+1}(x) \in \tilde{\mathcal{A}}^{\frac{C_2\Lambda_u^N}{\mathcal{I}^*}}$$

and $\mathcal{I}_k \geq \mathcal{I}^*$ for $k < n$ then the real orbit of x stays in upper chamber for the first n iterations and

$$(15) \quad |P_U^n(x) - G_U^n(x)| \leq \frac{C_2\Lambda_u^N}{\mathcal{I}^*}.$$

Next, set $C_3 = \frac{l_2^+ l_1^+}{l_2^- l_1^-} < 1$. Then during N iterations the value of I cannot drop by more than C_3^N times. Hence if x satisfies (14) and $\mathcal{I}_0 \geq C_3^N \mathcal{I}^*$

then (15) holds.

Now choose \mathcal{I}^* so that

$$(16) \quad \frac{C_2 \Lambda_u^N}{\mathcal{I}^*} < \delta$$

Now we consider the orbits where $\bar{\mathcal{I}} \leq \mathcal{I}_0 \leq \bar{\mathcal{I}} + 1$ for some $\bar{\mathcal{I}} \geq C_3^N \mathcal{I}^*$. There are three possibilities:

- (i) The real orbit of x leaves the upper chamber at some period $n < N$;
- (ii) The real orbit of x stays in $\tilde{\mathcal{A}}^\delta$ for the first N iterations;
- (iii) The real orbit of x stays in $\tilde{\mathcal{A}}^\delta$ until it hits $\mathcal{A}^\delta \cup (P_U^{12})^{-1} \mathcal{B}^\delta$ at some period $n < N$.

Proposition 6.3 and our choice of δ and \mathcal{I}^* imply that the set of orbits where either (ii) or (iii) happens has measure smaller than ϵ .

This completes the proof of Theorem 2. \square

7. CONCLUSION

We have described in this paper a two-dimensional exponential Fermi accelerator: a rectangular billiard with two moving slits. We found a mechanism for a particle to gain energy exponentially fast, i.e. the trapping regions. When the relative positions of two slits change at two critical jumps, a trapping region, either the upper or lower chamber, is created so that every high velocity orbit starts to gain energy exponentially fast once it gets trapped. We demonstrated that a trapping region exists for sizable choices of parameters and the exponential acceleration happens for almost all high energy orbits. Moreover under additional hyperbolicity assumptions on the parameters we provided an explicit estimate on the waiting time until which the exponential acceleration starts for most high-energy orbits.

It is worth noting that all the analysis done in this paper is based on the normal forms in the high energy region. The normal form implies exponential energy growth almost surely if a particle starts with sufficiently high initial velocity, and it eliminates the possibility of oscillatory orbits. The normal forms do not apply in low energy region where we might have bounded orbits for certain wall motion. In this paper we did not analyze the case when a trapping region does not exist, which can be easily achieved by choosing parameters such that the relative positions of two slits do not change at two critical jumps. Our normal forms still apply even in this complicated case but the analysis would be more delicate as the particle needs to make a choice of traveling up or down every time it jumps. We also note that in the non-resonant

case when the periods of the particle and the wall are incommensurable, the normal form still applies, however the jumping time depends on the period. In particular, the jumping times become dense on the period which precludes the existence of the trapping region, so the problem becomes similar to the resonant non-trapping case. These observations provide possible directions for future work.

REFERENCES

- [1] M. Arnold and V. Zharnitsky. Pinball dynamics: unlimited energy growth in switching Hamiltonian systems. *Comm. Math. Phys.*, 338(2):501–521, 2015.
- [2] J. De Simoi. Stability and instability results in a model of Fermi acceleration. *Discrete Contin. Dyn. Syst.*, 25(3):719–750, 2009.
- [3] J. De Simoi and D. Dolgopyat. Dynamics of some piecewise smooth Fermi–Ulam models. *Chaos: An Interdisciplinary Journal of Nonlinear Science*, 22(2):026124, 2012.
- [4] D. Dolgopyat. Lectures on bouncing balls. <http://www-users.math.umd.edu/~dolgop/BBNotes.pdf>.
- [5] D. Dolgopyat. Bouncing balls in non-linear potentials. *Discrete Contin. Dyn. Syst.*, 22(1-2):165–182, 2008.
- [6] D. Dolgopyat. Fermi acceleration. In *Geometric and probabilistic structures in dynamics*, volume 469 of *Contemp. Math.*, pages 149–166. Amer. Math. Soc., Providence, RI, 2008.
- [7] Krikorian R. Fayad, B. Hermans last geometric theorem. *Annales scientifiques de l’cole Normale Suprieure*, 42(2):193–219, 2009.
- [8] E. Fermi. On the origin of the cosmic radiation. *Phys. Rev.*, 75:1169–1174, Apr 1949.
- [9] V. Gelfreich, V. Rom-Kedar, K. Shah, and D. Turaev. Robust exponential acceleration in time-dependent billiards. *Physical review letters*, 106:074101, 02 2011.
- [10] V. Gelfreich, V. Rom-Kedar, and D. Turaev. Fermi acceleration and adiabatic invariants for non-autonomous billiards. *Chaos*, 22(3):033116, 21, 2012.
- [11] V. Gelfreich, V. Rom-Kedar, and D. Turaev. Oscillating mushrooms: adiabatic theory for a non-ergodic system. *J. Phys. A*, 47(39):395101, 21, 2014.
- [12] V. Gelfreich and D. Turaev. Fermi acceleration in non-autonomous billiards. *Journal of Physics A: Mathematical and Theoretical*, 41(21):212003, may 2008.
- [13] V. Gelfreich and D. Turaev. Unbounded energy growth in hamiltonian systems with a slowly varying parameter. *Commun. Math. Phys.*, 2008.
- [14] J. Koiller, R. Markarian, S.O. Kamphorst, and S.P. de Carvalho. Time-dependent billiards. *Nonlinearity*, 8(6):983–1003, nov 1995.
- [15] M. Kunze and R. Ortega. Escaping orbits are rare in the quasi-periodic Fermi–Ulam ping-pong. *Ergodic Theory and Dynamical Systems*, 2018.
- [16] S. Laederich and M. Lev. Invariant curves and time-dependent potentials. *Ergodic Theory and Dynamical Systems*, 11(2):365–378, 1991.
- [17] E.D. Leonel, J. Kamphorst, L. da Silva, and S.O. Kamphorst. On the dynamical properties of a fermi accelerator model. *Physica A: Statistical Mechanics and its Applications*, 331(3):435 – 447, 2004.

- [18] A. J. Lichtenberg, M. A. Lieberman, and R. H. Cohen. Fermi acceleration revisited. *Phys. D*, 1(3):291–305, 1980.
- [19] A. Loskutov, A. B. Ryabov, and L. G. Akinshin. Properties of some chaotic billiards with time-dependent boundaries. *Journal of Physics A: Mathematical and General*, 33(44):7973–7986, oct 2000.
- [20] R. Ortega. Boundedness in a piecewise linear oscillator and a variant of the small twist theorem. *Proc. London Math. Soc. (3)*, 79(2):381–413, 1999.
- [21] R. Ortega. Dynamics of a forced oscillator having an obstacle. In *Variational and topological methods in the study of nonlinear phenomena (Pisa, 2000)*, volume 49 of *Progr. Nonlinear Differential Equations Appl.*, pages 75–87. Birkhäuser Boston, Boston, MA, 2002.
- [22] L. D. Pustyl'nikov. Stable and oscillating motions in nonautonomous dynamical systems. II. *Trudy Moskov. Mat. Obšč.*, 34:3–103, 1977.
- [23] L. D. Pustyl'nikov. On Ulam's problem. *Theoret. and Math. Phys.*, 57:1035–1038, 1983.
- [24] L. D. Pustyl'nikov. Existence of invariant curves for maps close to degenerate maps, and a solution of the Fermi–Ulam problem. *Mat. Sb.*, 185:113–124, 1994.
- [25] K. Shah, D. Turaev, and V. Rom-Kedar. Exponential energy growth in a Fermi accelerator. *Phys. Rev. E*, 81:056205, May 2010.
- [26] S.M. Ulam. On some statistical properties of dynamical systems. In *Proceedings of the Fourth Berkeley Symposium on Mathematical Statistics and Probability, Volume 3: Contributions to Astronomy, Meteorology, and Physics*, pages 315–320, Berkeley, Calif., 1961. University of California Press.
- [27] V. Zharnitsky. Instability in Fermi-Ulam ping-pong problem. *Nonlinearity*, 11(6):1481–1487, nov 1998.
- [28] V. Zharnitsky. Invariant curve theorem for quasiperiodic twist mappings and stability of motion in the Fermi-Ulam problem. *Nonlinearity*, 13(4):1123–1136, 2000.